THE ASTROPHYSICAL JOURNAL, 402:493–513, 1993 January 10

EQUILIBRIUM SLAB MODELS OF LYMAN-ALPHA CLOUDS

JANE C. CHARLTON[1]
Steward Observatory, University of Arizona, Tucson, AZ 85721
EDWIN E. SALPETER
Space Sciences Building, Cornell University, Ithaca, NY 14853
AND
CRAIG J. HOGAN
Departments of Astronomy and Physics FM-20, University of Washington, Seattle, WA 98195

ABSTRACT

We model the Lyα clouds as slabs of hydrogen with an ionizing extragalactic radiation field incident from both sides. In general, the equilibrium configuration of a slab at redshift $z \lesssim 5$ is determined by a balance of the gas pressure, gravity (including the effects of a dark matter halo), and the pressure exerted by the intergalactic medium, P_{ext}. These models have been used to make predictions of the number of slabs as a function of the neutral hydrogen column density, N_H. A break in the curve is predicted at the transition between regimes where gravity and pressure are the dominant confining forces, with a less rapid decrease at larger N_H. The transition from optically thin to optically thick slabs leads to a gap in the distribution, whose location is governed largely by the spectrum of ionizing radiation.

Observations provide us with the distribution of N_H at $z \sim 2.5$, from the Lyα forest through the damped Lyα clouds. Recent HST data also provide a rough count of forest clouds at present and an indication of the rate of evolution. We define the prameters $\zeta \sim (1+z)^j$ and $P_{ext} \sim (1+z)^p$, representing the time-dependent ionization rate and external pressure. Comparisons with various observations are used to constrain these parameters, assuming that the population of clouds is described by a power-law distribution of total column densities: (1) The best fit is provided by $P_{ext}/k = 366$ cm^{-3} K near $z \sim 2.5$, based on the current observed value of the relative number of damped and forest clouds. If damped systems are undercounted due to dust obscuration, a smaller value of P_{ext}/k will result. (2) At $z \sim 2.5$ the number of Lyα forest clouds is observed to decrease rapidly, with the number $dN/dz \sim (1+z)^{2.4}$. This constrains the clouds to be pressure confined at that time, since gravity-confined clouds would evolve too slowly. (3) The large number of observed low z forest clouds (slower evolution since $z \sim 2.5$) requires a large value of P_{ext}/k and $j \gtrsim 3$. Gravity confinement may lead to evolution that is too slow, unless $j \lesssim 0$ or unless the gravity-confined clouds are mixed with some more rapidly evolving pressure-confined clouds. Combining the various arguments we find the best model has $P_{ext}/k \sim 1$ cm^{-3} K and $\zeta \sim 10^{-14}$ s^{-1} at present. Much smaller values of the pressure seem unlikely.

There are certain parallels between lines of sight through the outer HI disk of spiral galaxy with increasing radius, and the progression from damped, to Lyman limit, to forest clouds. We discuss briefly the possibility that at least some of the observed low z forest clouds may be a separate population, associated with galaxies, as suggested by the observations of Bahcall et al. This population could dominate the forest at present if the dark matter attached to galaxies should lead to gravity confinement for this disk population, while the isolated clouds remain pressure confined. The formalism developed in this paper will allow a more detailed study.

We also discuss a more general parameter study of the equilibrium configuration of slabs, including mock gravity and Lyα photon trapping. Although mock gravity on dust does not impact the analysis of Lyα clouds at $z \lesssim 5$, it may affect early growth of small scale structure at higher z.

Subject headings: hydrodynamics — quasars: absorption lines — radiative transfer

1. INTRODUCTION

Absorption lines shortward of Lyα emission in quasar spectra from $z \sim 5$ to the present indicate intervening clouds with neutral hydrogen column densities ranging over nine orders of magnitude (10^{13}–10^{22} cm^{-2}). The lowest column density, Lyα forest, clouds are usually thought to be highly ionized intergalactic material, but little is known observationally about specific properties of individual clouds. Clouds with larger neutral column densities are likely to be in some way associated with galaxies. These apparently different types of clouds may or may not be members of a single population formed by one mechanism. Their observational properties may serve as a cosmic "Rosetta Stone" for deciphering the link between the formation of galaxies and the evolution of the intergalactic medium.

In this paper, we will describe a general study of the equilibrium configuration of a slab of gas and dust, with radiation incident from both sides. The equilibrium is defined by the balance of the inward forces of gravity, continuum radiation pressure ("mock gravity"), and external pressure, and the outward forces of gas pressure and the trapping of Lyα photons. We shall show that in the case of Lyα clouds, the

[1] Present address: Davey Lab, Penn. State University, University Park, PA 16802.

equilibrium simplifies to a balance of gas pressure, and gravity or external pressure.

We will solve for the family of slabs that arise as equilibrium solutions when the incident ionizing radiation and the external pressure are uniform and isotropic. This will apply only to clouds that are isolated in the extragalactic background, rather than within galaxies, where incident radiation may not be isotropic and its intensity and spectrum may differ and where the pressure may increase due to coronal gas, or within clusters where the external pressure is surely higher. Our study of equilibrium configurations is similar to that of Black (1981), but for a slab rather than a spherical geometry, and including radiation pressure. It is of interest to study a slab geometry because it leads to greater flexibility in equilibrium models. Observations of clouds that appear in both lines of sight toward a lensed quasar (Smette et al. 1992) place lower limits of ~ 10 kpc on the transverse dimensions of Lyα clouds. In a slab geometry a thinner confined dimension can still be consistent with the data.

Rather than focus on a single model for cloud confinement, we will explore parameter space to find regimes in neutral H column density for which slabs are confined by gravity or by the pressure of the intergalactic medium (IGM). In the gravitational force we will include the effect of dark matter for various halo models. Since little is known about individual cloud properties, comparisons of model predictions are best made with the observed statistical properties of the cloud population. Two transitions between regimes (from optically thin to optically thick slabs and from gravitational to pressure confinement) lead to changes in the relationships between equilibrium cloud properties. Particularly important is the relationship between the neutral H column density $N_{\rm H}$ (an abbreviation for $N_{\rm HI}$) and the total H column density $N_{\rm tot}$. The latter is the quantity determined by the formation process, related to the total masses of clouds. The former can, at least in principle, be determined from observed spectra. The accuracy and method for this measurement are different for the different types of systems, but it is possible to tabulate a distribution function $f(N_{\rm H})$ of the number of clouds with a given $N_{\rm H}$ over the nine orders of magnitude in $N_{\rm H}$. As the relationship between $N_{\rm tot}$ and $N_{\rm H}$ changes through the various regimes we expect to see breaks or features in the observed $f(N_{\rm H})$. In this paper we will emphasize model predictions for the observed $f(N_{\rm H})$ in the hope that statistics and resolution will improve and allow uncontroversial detection of features or breaks.

The properties of the population of Lyα clouds change drastically with the pressure of the IGM. The clouds therefore provide a means to constrain this important, but unknown quantity. The questions of how much gas lies between the galaxies, and whether it is hot or cold, are central to understanding how galaxies formed. Processes that heat the IGM (i.e., explosions) presumably also act to reorganize the position of matter. A main theme throughout our discussion of Lyα cloud models will be their use in measuring the external pressure.

Recent *Hubble Space Telescope* (*HST*) observations (Bahcall et al. 1991, 1992, 1993; Morris et al. 1991) have yielded the first Lyα forest clouds seen at low redshift. There are more than expected from an extrapolation of the high z evolution downward. In at least a few cases, the low z forest clouds lie close to a galaxy (Bahcall et al. 1993), indicating a possible difference between high z and low z systems. The absolute number of clouds measured at $z \sim 0$ will be compared with model predictions for various choices of the magnitude and evolution of the IGM pressure and the extragalactic background radiation.

As the total column density of the disk of a spiral galaxy decreases with radius, we eventually expect a transition from an optically thick to optically thin regime. This transition has been observed as a break in the H I column density in the outer regions of a few spiral disks (Corbelli & Schneider 1990; Colgan, Salpeter, & Terzian 1990; Wakker, Vijfschaft, & Schwarz 1991, Carilli, van Gorkom, & Stoke 1989). It has been explored in detail by Corbelli & Salpeter (1993), with an emphasis on how the spectrum of radiation affects the shape of the break. Maloney (1993) has considered the detailed structure of the disk for the case of gravitationally confined slabs. We will complement these recent studies by considering how this data fits in with models of Lyα clouds, assuming that the pressure and ionization rate in the outer disk are comparable to the value elsewhere in the IGM.

Although not important for currently observable Lyα clouds, mock gravity on dust may affect early structure formation, possibly including the formation of Lyα clouds. Mock gravity (Spitzer 1941; Field 1971, 1976) leads to an attractive force, in the case of two particles via the mutual shadowing of radiation. The consequences of this instability for formation of large-scale structure have been discussed by Hogan & White (1986) and Hogan (1989). However, the lack of submillimeter background radiation in excess of blackbody effectively rules out such models for large-scale structure formation. We shall examine whether mock gravity can affect small-scale structure at very high z where constraints on the intensity of radiation are relaxed.

The organization of the paper is as follows. In § 2.1, we will summarize the current observational constraints on the radiation background at various times, and on the nature and evolution of the various types of Lyα systems. Then, in § 2.2, we mention previous theoretical work to establish what is the source of the background radiation and to model Lyα clouds. We begin § 3 by deriving the equation for pressure balance, assuming ionization equilibrium. This includes the forces of gravity, mock gravity, gas pressure, external pressure, and Lyα trapping. In § 3.1 we address the important question of whether such an equilibrium is stable. The regime with a dominant outward force contributed by trapping of Lyα photons is discussed in § 3.2. The possibility that structure formation at high z is affected by mock gravity is explored in § 4. We then proceed, in § 5, to the specific example of intergalactic clouds, for which the equilibrium is merely a balance of gas pressure, external pressure, and gravity. Section 5.1 gives general expressions for the equilibrium, including dark matter, assuming various relationships between the density of the dark matter halo and the total gas column density. The location of the transition between gravity and external pressure confined clouds sets a value of external pressure in terms of the other parameters. Another transition occurs as $N_{\rm H}$ is increased past the value for which slabs become optically thick to ionizing radiation. In § 5.2, we describe the effects these transitions have on the expected distributions of $N_{\rm H}$. We examine examples of where the first transition may occur (below, above, and in the Lyα forest) in § 5.3, and present figures illustrating the equilibrium behavior. In § 5.4, we compare model predictions to the data on the number of systems as a function of neutral column density, $f(N_{\rm H})$, and discuss constraints this may place on the external pressure. The evolution of the Lyα cloud population will depend on the changes in external pressure and in the

radiation field. Assuming a power-law distribution of cloud masses, the rate of evolution in the gravity and pressure dominated regimes is examined in § 6 and compared with the data. In § 7 we consider the outer region of the H I disk of spiral galaxies, and discuss the possible parallels with Lyα clouds. A summary and discussion follow in § 8.

2. CONSTRAINTS AND MODELS FOR BACKGROUND RADIATION, THE IGM, AND Lyα CLOUDS

2.1. *Observational Constraints*

We would like to know the full spectrum [intensity $J(\nu)$ in units of ergs s^{-1} cm^{-2} sr^{-1} Hz^{-1}] of the background radiation, however it is often easier to measure certain frequency-averaged quantities. We define the total energy flux, F, and density per steradian, u, of ionizing radiation (above $\nu_0 = 13.6$ eV) by

$$F = uc = \int_{\nu_0}^{\infty} J(\nu) d\nu \, . \tag{1}$$

The number flux of ionizing photons is given by

$$F_n = \int_{\nu_0}^{\infty} [J(\nu)/h\nu] d\nu \, . \tag{2}$$

Finally, the ionization rate, ζ, over 4π sr is defined as

$$\zeta = 6.3 \times 10^{-18} \int_{\nu_0}^{\infty} 4\pi \frac{J(\nu)}{h\nu} \left(\frac{\nu}{\nu_0}\right)^{-3} d\nu \, , \tag{3}$$

where we have used $\sigma_H = 6.3 \times 10^{-18}(\nu/\nu_0)^{-3}$ cm^{-2} for the photoionization cross section.

Let us examine a few simple examples of how these quantities would evolve. If all ionizing photons were created at a single time with a δ-function in energy, then $F \propto (1+z)^4$ and $\nu \propto (1+z)$. Therefore, as long as the photons are not absorbed, or shifted below the Lyman limit, the ionization rate ζ remains constant. We can generalize this to show that for any distribution of photons in energy and time, after the source is turned off no change in ζ will occur until some of the photons shift below 13.6 eV. If photons are created at some early time (large redshift z_0) with spectrum $J_0(\nu) \propto \nu^{-\alpha}$, then the spectrum $J(z, \nu)$ at $z < z_0$ is given by $J(z, \nu) = (1+z)^3 J_0[(1+z_0)\nu/(1+z)]$, and $\zeta \propto (1+z)^{3+\alpha}$.

We are particularly interested in observational constraints on UV radiation (or soft X-rays) capable of ionizing hydrogen. The number of ionizing photons from sources outside our galaxy is derived from the Hα surface brightness of high-velocity clouds (Kutyrev & Reynolds 1989) and yields a metagalactic number flux limit $F_n < 1.6 \times 10^4$ cm^{-2} s^{-1} sr^{-1}. This limit is considerably smaller than the flux measured by diffuse Hα emission and thought to be produced by a layer of warm ionized gas within our Galaxy ($F = 6 \times 10^5$ cm^{-2} s^{-1} sr^{-1}) (Reynolds 1990). Lower limits on the flux are given by Madau's (1992) estimate of the contribution of present-day quasars (taking into account attenuation by intervening galaxies) as $F = 4.0 \times 10^{-8}$ ergs cm^{-2} s^{-1} sr^{-1}, $F_n = 6.0 \times 10^2$ cm^{-2} s^{-1} sr^{-1}, and $\zeta = 1.6 \times 10^{-14}$ s^{-1}. The unattenuated value is a factor of 3 larger. The ionization time scale ζ^{-1} is considerably smaller than the Hubble time, so that ionization/recombination equilibrium will apply.

At higher z, an estimate of the ionizing background is given by the proximity effect: the decrease of abundance of Lyα forest clouds in the vicinity of a QSO. This yields a direct measurement of the ionization rate $\zeta = 2.7 \times 10^{-12}$ s^{-1}, roughly constant (within the uncertainty of an order of magnitude) in the range $1.7 < z < 3.8$. We will later focus on the redshift 2.5 as representative of Lyα forest cloud samples. If the spectrum is assumed to be $J(\nu) \propto \nu^{-1.5}$, as for quasars, this limit can be converted to an intensity $J_\nu = 10^{-21}$ in units of ergs cm^{-2} s^{-1} Hz^{-1} sr^{-1} at the ionization threshold of H (13.6 eV) (Bajtlik, Duncan, & Ostriker 1988). With this spectrum, the flux at intermediate redshifts is $F_n = 1.0 \times 10^5$ cm^{-2} s^{-1} sr^{-1} ($F = 6.6 \times 10^{-6}$ ergs cm^{-2} s^{-1} sr^{-1}), an order of magnitude larger than the upper limit on the present ionizing flux, and somewhat larger than the expected contribution by quasars at $z = 2.5$. Without any attenuation by intervening absorption-line systems Madau (1992) (assuming the same quasar spectrum) obtains $\zeta = 1.6 \times 10^{-12}$ s^{-1}, but for the more likely case with attenuation $\zeta = 3.5 \times 10^{-13}$ s^{-1}, considerably less than the proximity effect value.

Limits on ionizing radiaton at $z > 5$ are somewhat more vague. A UV photon from $z = 20$ will presently appear in the near IR at ~ 1 μm if it does not interact in the intervening space. However, it is quite likely (particularly in cases where mock gravity is important as we will see later) that the photon will be absorbed by dust and reemitted in the IR at a higher z. If this occurs early enough, the remnant radiation may be shifted into the submillimeter region by the present. The latter is accessible to the FIRAS experiment on *COBE*, and the former to DIRBE at 1 μm. The most recent FIRAS limit (Cheng 1991) is that over 3 to 20 cm^{-1} there is no deviation from a single-temperature pure blackbody spectrum more than 0.25% of the peak of the spectrum. Many theoretical models of galaxy formation are already threatened by this limit (Bond, Carr, & Hogan 1991), which is likely to improve by a factor of 2, assuming there is no detection of deviation. The conversion of this limit to an energy flux depends on assumptions about dust, but model 14 in Bond et al. is just permitted and yields 3.5×10^{-6} ergs cm^{-2} s^{-1} $sr^{-1}(1+z)^4$. The factor of $(1+z)^4$ implies that constraints are relaxed at high z. Present DIRBE limits are quite conservative due to the complications in modeling contributions from our Galaxy to the diffuse IR background. Currently, Hauser et al. (1990) give limits of $(2\text{–}3) \times 10^{-4}$ ergs cm^{-2} s^{-1} sr^{-1} in the regions 1–6 μm and 60–240 μm, and an order of magnitude less strict in the intermediate-wavelength range due to the interplanetary dust which has not been subtracted. Ultimately, these limits should improve drastically, but in the meantime it may be easier to "hide" cosmological background radiation in the far-IR than in the submillimeter. These limits also scale as $(1+z)^4$, but here z is the redshift at which the absorption by dust took place.

In summary, only at intermediate redshifts ($\sim$2–4) do we have a measurement of the level of extragalactic ionizing radiation. At larger z, and at smaller z, only upper limits exist. The present-day upper limits are, however, already smaller than the value at intermediate z.

The pressure P_{ext} of the IGM will be an important parameter for models of Lyα clouds. This parameter is, however, very weakly constrained because neither the density or the temperature of diffuse integalactic gas is known. Upper limits come from the production of an X-ray background (Lahav, Loeb, & McKee 1990) and the inverse Compton scattering of microwave background radiation off electrons (increased y parameter) that would result from a hot IGM (Mather et al. 1990). The latter, Sunyaev-Zeldovich effect provides the most

restrictive limit. The best limit from *COBE* is $y < 4 \times 10^{-4}$ (Cheng 1991). Since the distortion of the microwave background has contributions from many redshifts, the pressure limits at a particular z depend on its rate of evolution. Describing the evolution at $P_{ext} \sim (1 + z)^p$, for the case of adiabatic cooling ($p = 5$) we have $P_{ext} < 450[(1 + z)/3.5]^5$ cm^{-3} K, while for continuous shock heating ($p = 3.6$) (Ikeuchi & Ostriker 1986) the upper limit is $650[(1 + z)/3.5]^{3.6}$ cm^{-3} K. In setting these limits we have followed the same procedure as Ikeuchi & Turner (1991), but with the updated *COBE* limit. Limits at $z = 2.5$ are particularly relevant because observations of Lyα forest clouds are roughly centered around this z.

The absence of an absorption trough shortward of Lyα emission from distant QSOs indicates that very little uniformly distributed neutral H is present out to $z \sim 4.7$ (Schneider, Schmidt, & Gunn 1989). The most restrictive limit is given by Steidel & Sargent (1987) from a quasar at redshift 2.64, and yields an upper limit on the optical depth through neutral H, $\tau_{H\,I} < 0.02$. Assuming ionization/recombination balance for a given IGM temperature, this can be converted to an upper limit on the density in the IGM, Ω_{IGM} (expressed as a fraction of the critical density of the universe) (Madau 1992) and a corresponding upper limit on the pressure. For $T_{IGM} = 10^7$ K at $z = 2.64$ we obtain $\Omega_{IGM} < 0.29h_{75}^{3/2}$ or $P_{ext}/k < 923$ cm^{-3} K for $H_0 = 75$ km s^{-1} Mpc^{-1}. (We adopt this value of the Hubble constant for numerical examples throughout.) Similarly, $T_{IGM} = 10^6$ K implies $P_{ext}/k < 45$ cm^{-3} K ($\Omega_{IGM} < 0.14h_{75}^{3/2}$). Pressures as large as the *COBE* y-parameter upper limit are only possible with IGM temperatures at $z = 2.5$ in excess of 10^7 K. Larger densities, that could yield large P_{ext}/k for a smaller T_{IGM}, would violate the Gunn-Peterson limit on $\tau_{H\,I}$. We should also keep in mind that nucleosynthesis constrains the baryon density to $\Omega_b < 0.027h_{75}^2$ (Walker et al. 1991). Thus, to obtain a given pressure, an even larger temperature might be necessary. For such large temperatures ($> 10^6$ K) radiative cooling is unimportant, and the IGM will cool adiabatically unless there is additional heat input.

Now we shall proceed to discuss the observational properties of clouds of hydrogen from redshift 4 until the present. Lyα absorption is seen in QSO spectra from clouds with neutral H column densities, N_H, ranging from 10^{13} cm^{-2} to 10^{22} cm^{-2}. These are loosely divided into three groups: Lyα forest, Lyman limit, and damped Lyα systems. Ideally we would like to measure the two-dimensional distribution of clouds in N_H and z. However, a precise value of N_H can easily be obtained only in some ranges of N_H, and different methods are used in the various ranges. At the lower N_H end of the Lyα forest range, on the linear part of the curve of growth (10^{13}–10^{14} cm^{-2}), in principle, N_H values should be accurate, however, the effects of line blending (Barcons & Webb 1991) are difficult to estimate. For Lyman limit systems it is possible to obtain N_H from Lyα alone only if there is remnant radiation shortward of the Lyman limit ($N_H < 10^{17.7}$ cm^{-2}) (Lanzetta 1991). Somewhat larger values can be determined from higher resolution data that allow fitting of many Lyman series lines (Steidel 1990). For damped systems (10^{21}–10^{22} cm^{-2}), the profiles can be fit, and again accurate values can be obtained. Finally, even if all N_H values were known, there is not enough data to look at narrow ranges of N_H separately and find the redshift distribution as a function of N_H.

The Lyα forest clouds are the most numerous, with over 100 often seen in a single line of sight. They have N_H up to $\sim 10^{17}$ cm^{-2} (beyond which clouds become optically thick to radiation at the ionization threshold of H), no apparent correlations between the clouds, and close to primordial metal abundance ($\sim 0.1\%$ solar abundance of carbon, assuming $N_H/N_{tot} = 10^{-4}$, detected by Lu [1991], and similar limits on metals placed by Chaffee et al. [1986]. (Since the observed quantity is the metal abundance relative to neutral H, the model dependent ratio N_H/N_{tot} enters into the derivation of metallicity relative to solar.) The distribution of the number of clouds as a function of column density has often been claimed to follow a single power law $f(N_H) \propto N_H^{-\beta}$, where β is typically ~ 1.5–1.7 (Carswell et al. 1984; Atwood, Baldwin, & Carswell 1985; Tytler 1987). Recently, however, the collection of lower N_H column density data, along with the application of a new technique to infer the column density from the line-width, led Jenkins, Bajtlik, & Dobrzycki (1992) (see Jenkins & Ostriker 1991) to suggest a double power law with a break at $N_H \sim 3 \times 10^{13}$ cm^{-2}:

$$f(N_H) \propto N_H^{-1.3}\left[1 + \left(\frac{N_H}{3 \times 10^{13}}\right)^{-0.7}\right]. \quad (4)$$

Webb et al. (1992) have also suggested that a different power law applies below $N_H \sim 5 \times 10^{13}$ cm^2, however, their slope changes in the opposite direction. (They do alternatively suggest that the observed opacity could be fitted with a significant Gunn-Peterson effect.) Therefore, it appears that these results are still quite controversial.

The number of clouds with a given N_H evolves as $(1 + z)^{2.36 \pm 0.4}$ at $4 > z > 2$ (Bajtlik, Duncan, & Ostriker 1988); however, Bechtold (1993) is finding that this depends on equivalent width limits. This must be compared to the value expected if the number of sources in a comoving volume is fixed. The number of clouds observed in an interval dz is then the product of the actual density, the fixed cloud cross section, and the proper length in that interval (Sargent et al. 1980) so that

$$dN/dz \propto (1 + z)/(1 + \Omega_0 z)^{1/2}. \quad (5)$$

This yields a power law $dN/dz \propto (1 + z)$ for $\Omega_0 = 0$, and $dN/dz \propto (1 + z)^{1/2}$ for $\Omega_0 = 1$.

Recent HST observations have yielded the absolute number of forest clouds at present. For equivalent widths larger than 0.32 Å, the number per unit redshift is $dN/dz|_0 = 15 \pm 4$, obtained by combining lines of sight toward 3C 273, H1821+643, and PKS 0405−12 (Bahcall et al. 1993). For typical Doppler parameters of 35 km s^{-1}, the neutral column density corresponding to this equivalent width is $N_H = 6.3 \times 10^{13}$ cm^{-2}. If the evolution of these clouds since $z \sim 2.5$ is fit by a single power law $dN/dz \propto (1 + z)^\Gamma$, the result is $\Gamma = 0.8$, consistent with cosmological evolution (eq. [5]) for either value of Ω_0, from $z = 2.5$ until the present (Bahcall et al. 1991; Morris et al. 1991). Note, however, that this will only match cosmological evolution if there is no change in the pressure or ionization rate over this time interval.

The only clue about the geometry and physical size of clouds (and thus their degree of ionization) comes from clouds appearing in two different lines of sight to a lensed system (Smette et al. 1992). This yields a transverse dimension larger than $12h_{50}^{-1}$ kpc. Except for very low external pressure, models then suggest that this dimension may be significantly larger than that along the line of sight, indicating a slab rather than a spherical cloud.

The measurement of line profiles of Lyα in high-resolution spectra (Pettini et al. 1991; Carswell et al. 1991) allow estimates

of cloud temperatures. The original suggestion by Pettini et al. (1991) that $T < 10{,}000$ K in low N_H systems is called into question by the identification of many lines with metals from newly detected Mg II systems (Bechtold 1991) and by the analysis of Rauch et al. (1992). A definite Lyα forest identifications are consistent with $T > 10{,}000$ K, and range up through 30,000 K (line width 22 km s^{-1}) if line broadening is due purely to thermal motions.

Lyman-limit systems are optically thick to radiation with energy 13.6 eV ($\log N_H > 17.2$). In the range $17.2 < \log N_H < 21.8$, Lanzetta (1991) has fitted the data by a power law, $f(N_H) \propto N_H^{-1.25 \pm 0.03}$. The exponent is appreciably smaller, but barely consistent (within errors) with a continuation of the Lyα forest on the high N_H end. With this power-law relation, 75% of all systems with $\log N_H > 17.2$ would have log 17.2 would have $\log N_H > 17.7$.

There is disagreement between the two observational results on the evolution of Lyman limit systems. Lanzetta (1991) claims that the Lyman limit systems evolve strongly ($dN/dz \propto (1+z)^\Gamma$, where $\Gamma = 5.7 \pm 1.9$) for $z > 2.5$, and below $z \sim 2.5$ the comoving density of clouds per unit z is constant. Steidel's private communication [Steidel 1991] result, however, is that $\Gamma = 1.1 \pm 0.4$ over the range $4 > z > 0.4$, and $\Gamma = 1.6 \pm 1.9$ for $z > 2.5$. Many of the Lyman limit systems (and perhaps all) contain metals and are in some cases coincident with members of C IV–selected (Sargent, Boksenberg, & Steidel 1988; Steidel 1990) or Mg II–selected (Lanzetta, Turnshek, & Wolfe 1987; Sargent, Steidel, & Boksenberg 1989) samples. Ratios of abundances of various ionized species allow a probe of conditions in the clouds and constraints on background radiation (Steidel 1990; Madau 1991).

Finally, damped Lyα systems arise if N_H is large enough that scattering of Lyα occurs in the damping wings ($\log N_H > 20.8$). It is again possible to measure N_H and the distribution is $f(N_H) \propto N_H^{-1.7}$ within the damped Lyα regime (Lanzetta 1991), although the normalization is somewhat different than for the forest clouds. This difference in normalization is important and will be discussed in § 5.4. These systems at $z > 2$ have been estimated to have metal abundances $\sim 10\%$ of solar (Pei, Fall, & Bechtold (1991).

To summarize the properties of clouds: The distribution of the number of clouds is roughly a power law $f(N_H) \propto N_H^{-1.7}$ over 10 decades in N_H. However, deviations from this power law can be significant and elude detection in present data, particularly in the Lyα forest and in the range $17.7 < \log N_H < 20.8$.

2.2. *Theoretical Ideas*

In this section, we shall first briefly discuss possible sources of ionizing radiation and then review existing models of Lyα clouds. It appears that in order to produce the proximity effect above $z \sim 2.5$, and well as to satisfy the Gunn-Peterson test, radiation in excess of that produced by observed quasars is needed (Bechtold et al. 1987; Shapiro & Giroux 1987; Miralda-Escude' & Ostriker 1990). Plausible sources include radiation from primordial galaxies and from obscured quasars (Miralda-Escude' & Ostriker 1990). Although there have been objections that high-mass stars have a spectrum too soft to fit the ionization states of metal line systems, Madau (1991) pointed out that the Lyα clouds act as intervening absorbers and harden the spectrum.

The key questions with regard to the Lyα forest clouds are (1) What is the degree of ionization and thus the contribution to Ω, and what is the metallicity? (2) What is the mechanism for confinement and stability? (3) How do they evolve? It is impossible to determine the answers directly from observations since all that is known is, at best, N_H, b, and a limit on the transverse dimension. Since the clouds are not correlated in their positions at high z they are thought to be separate from ordinary galaxies (although there may be some correlation with galaxies at lower z; Bahcall, et al. 1992). The mass in this component can be negligible if clouds are neutral or comparable to that in galaxies in they are extremely ionized. Many early models assume spherical clouds and find them to be highly ionized (e.g., Sargent et al. 1980; Black 1981). Later, models in which clouds are largely neutral, dense sheets (Hogan 1987; Baron et al. 1989), cloudlets (Lake 1988), or elongated spheroids (Barcons & Fabian 1987) were proposed. The geometry can provide a clue as to whether structure formation occurred as fragmentation from sheets (Vishniac & Bust 1987), or as hierarchical build-up (Rees 1986). Recent simulations (Ostriker, private communication [Cen & Ostriker 1991]) indicate that sheets are the probable geometry in many dark matter models.

Perhaps the most visible debate concerns the mechanism of confinement. Clouds confined by self-gravity alone are likely to be Jeans unstable and may have implausible parameters. This led Sargent et al. (1980) to propose confinement by the pressure of a hot IGM (Ostriker & Ikeuchi 1983; Ikeuchi & Ostriker 1986) and Rees (1986) to suggest clouds embedded in CDM halos. Bond, Szalay, & Silk (1988) and Duncan, Vishniac, & Ostriker (1991) have discussed models in which clouds are not static, but freely expanding. These models yield lower cloud temperatures and predict a positive correlation between N_H and equivalent width. Spheres with radii as large as the transverse dimension must have very low confining pressures and very high degrees of ionization, thus large masses. There is then an even more serious problem with Jeans instability. Sheets do not place such requirements on the pressure and thus may be better in this respect.

Williger & Babul (1992) have undertaken hydrodynamic simulations that address the effect of an upper mass cutoff for pressure-confined spherical clouds. Such a cutoff leads to a deficiency of large column density clouds at low redshift (as the clouds become more neutral and the cutoff shifts downward in N_H). They also suggest that aspherical systems may provide a resolution to the discrepancy.

The observation of more Lyα forest clouds than predicted by an extrapolation of the power law that holds at higher z has been addressed theoretically in two recent papers (Fukugita & Lahav 1991; Ikeuchi & Turner 1991). In the context of a pressure-confined model with an adiabatically expanding IGM, the former emphasize the importance of the cosmological model in determining changes in the number of clouds with z. The latter, also in a pressure-confined model, conclude that the observed evolution is consistent with the observed emissivity of quasars (increasing out to $z \sim 2$, then leveling off). We will consider evolution in a more general context.

One important issue concerning the transition to Lyman limit systems is whether there is an increase in metallicity at the same N_H. Some of these systems must be associated with galaxies, since they exhibit metal lines, but it is not clear if there is a separate population of 10^{17} cm$^{-2} < N_H < 10^{20}$ cm^{-2} clouds, or whether they are all lines of sight through larger galaxies. Finally, many damped Lyα systems (Lanzetta et al. 1991) are likely to correspond to lines of sight through proto-

galaxies or young galaxies (Lanzetta et al. 1991; Womble, Junkkarinen, & Burbidge 1992).

The next section is a general discussion of slab equilibria, followed by § 4, an application to structure growth by mock gravity. The reader who is primarily interested in Lyα clouds can skip to a self-contained discussion beginning in § 5.

3. EQUILIBRIUM CONFIGURATION OF A SLAB

In order to obtain analytic expressions, we make various simplifying assumptions for a slab of total column density (neutral plus ionized hydrogen) $N_{\rm tot}$. We idealize the geometry as an infinite slab with uniform total number density $n_{\rm tot}$ and a sharp edge at a distance $W/2$ (half the slab width, W) from the center, where $n_{\rm tot} = N_{\rm tot}/W$ represents the typical density and $W/2$ is of the order of a scale height. The column density and density of H in the neutral form are denoted $N_{\rm H}$ (short for $N_{\rm H\,I}$) and $n_{\rm H}$. For most purposes, we assume the slab is composed of only H (no He) and of dust with abundance g_D expressed in terms of magnitudes of extinction by absorption at 13.6 eV in our galaxy per $N_{\rm tot}$ (1.1×10^{-21} mag cm^2; Black 1991). (We have used $N_{\rm H}/A_V = 1.6 \times 10^{21}$ cm^{-2} mag^{-1} for the gas/extinction ratio, $A_{13.6\,\rm eV}/A_V = 5.27$ and assumed that at this energy 35% of the total extinction is due to absorption.) The product $g_D N_{\rm tot}$ in the slab gives the optical depth to absorption by dust at the Lyman edge. We will leave the equilibrium temperature as a free parameter, T, assumed to be constant throughout the slab. Dark matter is characterized by the ratio of total mass (sum of dark matter and gas) to gas mass, η, which is a function of $N_{\rm tot}$. Radiation incident upon the slab is taken to be isotropic, and is characterized by the ionization rate ζ (defined in eq. [3]). In some cases we will take it to be a δ-function at a particular energy E_γ with energy density per steradian u (defined in eq. [1]). This idealized case will illustrate the effects of changing the spectrum. In other situations we shall use a more realistic, quasar-like spectrum ($J \propto \nu^{-\alpha}$ where $\alpha \sim 1.5$). Finally, the medium external to the slab is characterized by its temperature $T_{\rm ext}$ and its density $\Omega_{\rm ext}$ in units of the critical density $\rho_{\rm crit}$, and is assumed to be uniform and isothermal. The external pressure, $P_{\rm ext}$, is given by

$$\frac{P_{\rm ext}}{k} = 2.8 \times 10^{-4}\ {\rm cm^{-3}\ K}\ \Omega_{\rm ext}\, T_{\rm ext}\left(\frac{1+z}{3.5}\right)^3 . \tag{6}$$

We now proceed to find a general expression for the equilibrium state of the idealized slab in terms of the input parameters $N_{\rm tot}$, T, ζ, g_D, E_γ, $\Omega_{\rm ext}$, and $T_{\rm ext}$. First, we require the slab to be in ionization equilibrium:

$$\zeta n_{\rm H} = \alpha_{\rm rec}\, n_{\rm tot}^2 \tag{7}$$

where $\alpha_{\rm rec} = 4.07 \times 10^{-13}$ cm^3 s^{-1} $(T/10{,}000\ {\rm K})^{-0.75}$ is the recombination coefficient. Collisional ionization is not important compared to photoionization for low temperatures (10,000–30,000 K) and low densities. It is safe to assume that photoionization is dominant for parameters relevant to Lyα clouds. Now we shall consider the slab as two identical half slabs and calculate the various forces acting in the problem.

The inward gravitational force (all forces throughout expressed per unit area) on the half column with column density $N_{\rm tot}/2$ is given by

$$F_{\rm gr} = \frac{\pi}{4} G m_{\rm H}^2 N_{\rm tot}^2 \eta(N_{\rm tot}) , \tag{8}$$

where $m_{\rm H}$ is the mass of H. We have assumed that the slab is mostly ionized so that the mean mass of an individual particle is $m_{\rm H}/2$, but the total column density (including electrons) is twice $N_{\rm tot}$. An additional inward force will be exerted by a hot external medium:

$$F_{\rm ext} = 2\Omega_{\rm ext} \frac{\rho_{\rm crit}}{m_{\rm H}} kT_{\rm ext} . \tag{9}$$

The outward force due to gas pressure is also simply given as

$$F_{\rm gas} = 2n_{\rm tot}\, kT . \tag{10}$$

The forces due to radiation can be classified as two types: those due to radiation incident from outside the slab, and those due to internally produced photons.

Consider the momentum imparted to the slab by the incident radiation of energy E_γ. We can compute the radiation pressure on the edge, $P(W/2)$, and on the center, $P(0)$, of the slab and subtract to find the force (pressure gradient) on the half slab. First, consider the inward force contributed by absorption of the incident radiation (either by neutral H [photoionization] or by dust). The optical depth for normal incidence of the photons is $\tau_{\rm abs} = N_{\rm abs}\sigma_{\rm abs}$, where $\sigma_{\rm abs}$ is the cross section for absorption and $N_{\rm abs}$ is the column density of absorbers. We can express the results in terms of the pressure P_0 that would result (integrating over all angles) if there were no absorbers in the slab:

$$P_0 = \int_{-1}^{1} u\mu^2 d\mu = (\tfrac{2}{3})u . \tag{11}$$

Then the pressure at the left edge of the slab can be written as

$$P(z_1) = (\tfrac{1}{2})P_0 + \int_{-1}^{0} u\, \exp^{(\tau_{\rm abs}/\mu)} \mu^2 d\mu . \tag{12}$$

Similarly, at the slab center

$$P(0) = 2\int_0^1 \exp^{-\tau_{\rm abs}/2\mu} \mu^2 d\mu . \tag{13}$$

The net inward force, expressed in dimensionless form, is then

$$\begin{aligned} f'(\tau_{\rm abs}) &= [P(z_1) - P(0)]/P_0 \\ &= (\tfrac{3}{2})\int_0^1 (1 - \exp^{-\tau_{\rm abs}/2\mu})^2 \mu^2 d\mu , \end{aligned} \tag{14}$$

which reduces to

$$f'(\tau_{\rm abs}) = (\tfrac{3}{8})\tau_{\rm abs}^2 \quad \text{for } \tau_{\rm abs} \ll 1 , \tag{15a}$$

$$f'(\tau_{\rm abs}) = \tfrac{1}{2} \quad \text{for } \tau_{\rm abs} \gg 1 . \tag{15b}$$

Next we shall consider the force exerted on the half slab by an isotropic distribution of photons produced in the slab. This will apply to the Lyα photons produced in recombinations or to photons scattered by neutral H or dust. Define χ as the emissivity (in ergs cm^{-4} sr^{-1}) for these photons alone. For Lyα photons, $\chi = n_\gamma n_{\rm H} \sigma_{\rm H} E_{{\rm Ly}\alpha}/4\pi$, where n_γ is the number density of incident ionizing photons. Now we shall assume the optical depth to scattering $\tau_{\rm sc} \ll 1$. Since all photons must ultimately escape, the pressure due to photons at the slab edge z_1 is the same as the pressure $P_{\rm sc0}$ in the absence of scattering:

$$P_{\rm sc}(z_1) = P_{\rm sc0} = \int_{-1}^{1} \mu^2 d\mu \int_0^{W/2} \chi dx = (\tfrac{1}{3})\chi W . \tag{16}$$

The pressure at slab center is obtained by considering the additional contribution of photons back-scattered through the center and subtracting the photons that back-scatter before reaching slab center. Integrating over μ, and assuming the distribution in μ is isotropic, we obtain

$$P_{sc}(0) = (\tfrac{1}{3})\chi W + (\tfrac{1}{8})\tau_{sc}\chi W . \quad (17)$$

As in the case of absorption of incident radiation, we define

$$f'_{sc} = [P_{sc}(0) - P_{sc}(z_1)]/P_{sc0} = (\tfrac{3}{8})\tau_{sc} . \quad (18)$$

In the case of Lyα photons produced within the slab (for $\tau_{Ly\alpha} \ll 1$), $f'_{Ly\alpha} = f'_{sc}(\tau_{Ly\alpha}) = (\frac{3}{8})N_H k_0$, where $k_0 = 8 \times 10^{-14}(T/10{,}000\ \mathrm{K})^{-1/2}$ cm^2.

The scattering of continuum photons (either by dust or by Thomson scattering by electrons) in an optically thin medium will contribute no net force on a half slab. We can see this by treating the first scatterings of incident photons as absorptions followed by the production of an isotropic field within the slab. The two contributions cancel. This is also a consequence of Liouville's theorem.

For a slab optically thick to the Lyα photons, we cannot compute the force analytically. The pressure on the outer edge $P_{sc}(z_1)$ must still be P_{sc0}, since the Lyα photons will continue to be absorbed and reemitted until they escape. $P_{sc}(0)$ is now determined by the number of times a photon passes through the center before escaping. Bonilha et al. (1979) have fitted the expression

$$\frac{L_0}{\tau} = 1 + \frac{2\ln\tau}{(1 + 0.3a\tau)^{2/3}} + (6.5a\tau)^{1/3} \quad (19)$$

for the path length covered by an escaping photon that was produced at optical depth τ in a plane-parallel slab. The quantity a is the damping constant ($=4.7 \times 10^{-4}$ for Lyα) so that when $a\tau \ll 1$, scattering occurs within the Doppler wings, and a photon will escape when it scatters to a frequency for which the optical depth is less than unity. For this case $L_0/\tau = 1 + 2\ln\tau$ and $P_{sc}(0) = [1 + 2\ln(\tau_{Ly\alpha}/2)]P_{sc0}$. Thus for $1 \ll \tau_{Ly\alpha}/2 \ll a^{-1}$, $f'_{Ly\alpha} = 2\ln(\tau_{Ly\alpha}/2)$. When $a\tau_{Ly\alpha}/2 \gg 1$ the force is given by $f'_{Ly\alpha} = [6.5a(\tau_{Ly\alpha}/2)]^{1/3}$. This assumes, however, that the optical depth to the incident photons is less than 1 ($N_H\sigma_H < 1$). Since $\tau_{Ly\alpha}/\tau_H = 1.2 \times 10^4(T/10{,}000\ \mathrm{K})^{-0.5}(E_\gamma/13.6\ \mathrm{eV})^3$, this will occur at close to the same $\tau_{Ly\alpha}$ that the damping wings become important. The case which is optically thick to the incident continuum will take a different form: that of a sandwich, with a central neutral region.

The above discussion yields the following expressions for the inward mock gravity and outward Lyα trapping forces:

$$F_{mock} = (\tfrac{2}{3})uf'_{abs}(\tau) = u\tau_{abs}^2/4 \quad \tau_{abs} \ll 1 , \quad (20a)$$

$$= (\tfrac{1}{3})u \quad \tau_{abs} \gg 1 ; \quad (20b)$$

$$F_{Ly\alpha} = (2/3)u\tau_H f'_{Ly\alpha}(\tau_{Ly\alpha})(E_{Ly\alpha}/E_\gamma) , \quad (21a)$$

$$= (u\tau_{Ly\alpha}\tau_H/4)(E_{Ly\alpha}/E_\gamma) , \quad \tau_{Ly\alpha} \ll 1 ; \quad (21b)$$

$$= (4/3)u[\ln(\tau_{Ly\alpha}/2)]\tau_H(E_{Ly\alpha}/E_\gamma) , \quad 1 \ll \tau_{Ly\alpha} \ll a^{-1} ; \quad (21c)$$

$$= (2/3)u[6.5a(\tau_{Ly\alpha}/2)]^{1/3}\tau_H(E_{Ly\alpha}/E_\gamma) , \quad \tau_{Ly\alpha} \gg a^{-1} . \quad (21d)$$

It is now clear that in all cases the inward force of mock gravity on neutral H is dominated by the outward force contributed by the trapped Lyα photons (since $\tau_{Ly\alpha} \gg \tau_H$). This is not necessarily the case, however, with mock gravity on dust since the absorbed photon is shifted to the infrared.

The final balance of forces can be written as

$$\kappa\left[\eta + \left(\frac{u}{u_0}\right)g_D^2\right]\left(\frac{N_{tot}}{N_0}\right)^2 + \frac{F_{ext}}{F_0} = \left[1 + \left(\frac{2}{3}\right)\left(\frac{N_{tot}}{N_0}\right)f_{Ly\alpha}(\tau_{Ly\alpha})\right]\left(\frac{n_{tot}}{n_0}\right) \quad (22)$$

for a slab that is optically thin through neutral H and through dust (but not necessarily through Lyα). We have written this in a convenient form by defining units as follows:

$$u_0 = \frac{\pi G m_H^2}{(1.1 \times 10^{-21})^2} = 4.8 \times 10^{-13}\ \mathrm{ergs\ cm^{-3}\ sr^{-1}} ; \quad (23a)$$

$$N_0 = \frac{kT}{E_{Ly\alpha}}\frac{8\pi c}{\alpha_{rec}} = 1.6 \times 10^{23}\ \mathrm{cm^{-2}}\left(\frac{T}{10{,}000\ \mathrm{K}}\right)^{1.75} ; \quad (23b)$$

$$n_0 = \frac{4\pi c}{\alpha_{rec}}\frac{\sigma_H}{k_0}\frac{u_0}{N_0 E_\gamma} = 9.9 \times 10^{-6}\ \mathrm{cm^{-3}} \times \left(\frac{T}{10{,}000\ \mathrm{K}}\right)^{-0.5}\left(\frac{E_\gamma}{13.6\ \mathrm{eV}}\right)^{-4} ; \quad (23c)$$

$$F_0 = 2kTn_0 = 2.7 \times 10^{-17}\ \mathrm{g\ cm\ s^{-2}} \times \left(\frac{T}{10{,}000\ \mathrm{K}}\right)^{0.5}\left(\frac{E_\gamma}{13.6\ \mathrm{eV}}\right) . \quad (23d)$$

The definition of u_0 is such that for $g_D = 1$, and $\eta = 1$, at $u = u_0$ the inward forces of gravity and of mock gravity are equal. For $N = N_0$, the outward Lyα and gas pressures contribute equally when $\tau_{Ly\alpha} = 1$. If $\eta = 1$, gravity and external pressure will contribute equally for $F_{ext} = \kappa F_0$. The total density n_{tot} is expressed in terms of n_0 in order that

$$\tau_{Ly\alpha} = \left(\frac{N_{tot}}{N_0}\right)\left(\frac{n_{tot}}{n_0}\right)\left(\frac{u_0}{u}\right) . \quad (24)$$

With these definitions,

$$\kappa = \frac{\pi G m_H^2 N_0^2}{4F_0} = 1.4 \times 10^8\left(\frac{T}{10{,}000\ \mathrm{K}}\right)^3\left(\frac{E_\gamma}{13.6\ \mathrm{eV}}\right)^4 . \quad (25)$$

This notation facilitates easy comparison between the terms.

3.1. *Stability*

We have just written a general specification of the equilibrium configuration of a slab (assuming that the width, W, is considerably smaller than the distance sound would travel in a Hubble time). This equilibrium, however, is meaningless unless it is stable. We can write equation (22) in terms of only W and N_{tot} of the slab. Since N_{tot} remains constant in a contraction or expansion, we can determine by inspection if we have stability in the sense that a contraction will not lead to collapse, and an expansion will not lead to continued expansion. First, note that since $\tau_{Ly\alpha} \propto N_{tot}^2/W$, $f'_{Ly\alpha}$ decreases with increasing W for all $\tau_{Ly\alpha}$. Thus the left-hand side of equation (22), the inward force, remains constant in an expansion or contraction; however, the outward force will always adjust back toward equilibrium (since W appears in the denominator). This uses the fact that ionization/recombination balance is reestablished on a time scale that is short compared to that for expansion or contraction. So regardless of which of the forces is dominant, the thin dimension of the slab is stable to this simple perturbation.

We must also consider Jeans instabilities in the long dimension. If gravity is the dominant inward force, the Jeans length is by definition the width, W. Thus the slab is unstable to perturbations with wavelength $\lambda > W$. Several effects, however, may prevent such an instability: (1) An outward force along the long dimension would be produced by a rotating slab. The condition for a stable sheet is (Binney & Tremaine 1987)

$$\frac{v_s v_{\rm rot}}{G m_{\rm H} N_{\rm tot} R} \geq \frac{\pi}{4}, \tag{26}$$

where v_s is the sound speed and $v_{\rm rot}$ is the rotation velocity. For sheet radius $R = 30$ kpc and $v_s = 9$ km s^{-1} ($T = 10{,}000$ K) this yields

$$v_{\rm rot} > \left(\frac{N_{\rm tot}}{2 \times 10^{19}\ {\rm cm}^{-2}}\right) {\rm km\ s}^{-1}, \tag{27}$$

so it is not implausible to have rotational support. (2) Bulk turbulent motion can increase the gas pressure sufficiently that the long dimension will not collapse. (3) If the external pressure dominates, W can be reduced below the Jeans length. In this case it is possible that the Jeans length exceeds the long dimension (tens of kiloparsecs). Then this dimension may also be stable. A confining dark matter halo may have a similar effect. (4) The age of the slab could be less than the collapse time scale in the longer direction so that a given slab is a transient phenomenon. For observed velocity dispersions of 10–20 km s^{-1}, the dynamical time scale $(GN_{\rm tot} m_{\rm H}/2R)^{-1/2}$ exceeds a Hubble time for $R > 150\ (1+z)^{-3/2}$ kpc. Thus, at $z \sim 2.5$ for example, we can consider explicitly only cases where the slab equilibrium width $W_{\rm eq} \ll 20$ kpc.

A spherical gas cloud with gravity alone (and no dark matter) will be unstable due to a gravitational force falling off like $1/r^2$ (increasing more rapidly than the gas pressure under compression). Since observable constraints on the size (from QSO pairs) refer to the long dimension, slab models allow the line of sight dimension to be smaller than spherical models and therefore a wider range of equilibria can be found consistent with observations. In addition, if clouds form from hydrodynamical processes (rather than gravitation) slabs are a more natural geometry to expect.

3.2. *Conditions for* Lyα *Trapping Force to Enter*

If the force due to trapped Lyα photons is to exceed the gas pressure, from equation (22), the condition

$$(2/3)(N_{\rm tot}/N_0) f'(\tau_{\rm Ly\alpha}) > 1 \tag{28}$$

must be satisfied. For $\tau_{\rm Ly\alpha} \ll 1$, $f'(\tau_{\rm Ly\alpha}) = (3/8)\tau_{\rm Lya}$ and only for $N_{\rm tot} > 4N_0/\tau_{\rm Ly\alpha}$ will Lyα pressure contribute. This would occur only for implausibly large $N_{\rm tot}$ (larger than the largest galaxy).

When we pass into the regime where the slab is optically thick to Lyα the condition becomes somewhat less severe. The requirement of dominant Lyα yields $N_{\rm tot} > (3/4)N_0/[\ln(\tau_{\rm Ly\alpha}/2]$, still larger than a dense spiral galaxy ($\sim 2 \times 10^{22}$ cm^{-2}) for all $\tau_{\rm Ly\alpha}$ less than α^{-1}. Once the wings become important the condition becomes $N_{\rm tot} > (13/\tau_{\rm Ly\alpha}^{1/3})N_0$. Since the $\tau_{\rm Lya}$ dependence is weaker this still requires very large total column densities. Also, as we increase $\tau_{\rm Ly\alpha}$, $\tau_{\rm H}$ is also increased and is larger than unity for $\tau_{\rm Ly\alpha} > 1.2 \times 10^4 (T/10{,}000\ {\rm K})^{-0.5}\ (E_\gamma/13.6\ {\rm eV})^3$. After this transition we enter a separate regime with a neutral slab center. Thus it is only for high energies that we are likely to see a slab that is optically thin to continuum photons, in which Lyα photon trapping is important. This effect is important only for a small range of parameter space. In future sections we shall concentrate on the more probable case where $F_{\rm gas} \gg F_{\rm Ly\alpha}$.

Braun & Dekel (1989) have also examined the effect of the pressure of trapped Lyα photons in the slab geometry. They present an expression for the ratio of the Lyα pressure to the gas pressure, that depends both on the slab width and the total density. Their Figure 1 illustrates the region of the phase space of $n_{\rm tot}$ and W for which the trapping force can be significant (small width and high density). Our results are in agreement with theirs, but we are working in a somewhat different context. In equilibrium, there is a direct relationship between density and width. We find therefore, that in equilibrium the density is always too small for the trapping force to dominate. If an unstable slab has collapsed to a denser state, the Lyα photons could eventually halt the collapse as Braun & Dekel describe.

4. SPECULATIVE POSSIBLE ROLES OF MOCK GRAVITY IN EARLY STRUCTURE FORMATION

From equation (22) we find that mock gravity has a significant effect only if $(u/u_0)g_D^2 \gtrsim \eta$. Even for $g_D = 1$ this would require $u \gtrsim 4.8 \times 10^{-13}\eta$ ergs cm^{-3} sr^{-1}, which is orders of magnitude larger than the value given by the proximity effect. Dust can absorb radiation with energies less than the Lyman edge, as well as ionizing radiation. As the wavelength is increased the cross section for absorption is expected to decrease, however, for some types of spectra of incident radiation the contribution from absorption in the optical can be significant. For example, if we take $J_\nu \propto \nu^{-1.5}$ the contribution to the optical depth for radiation up through 5000 Å is a factor of 2.3 larger than the contribution from UV and X-rays alone. The correction could be somewhat larger for a stellar spectrum. However, even including this factor, it is clear that mock gravity does not contribute to slab equilibria at currently observable redshifts. As discussed in § 2.1, constraints on higher z radiation depend on whether it is absorbed by dust and shifted to the IR. The FIRAS and DIRBE limits translate to $u < 8 \times 10^{-5}\ (1+z)^4 u_0$ and $u < 6 \times 10^{-3}\ (1+z)^4 u_0$, respectively, in the appropriate wavelength regimes. Using the FIRAS limit (assuming absorption by dust does occur), we see that for $g_{\rm D} = 0.01$ and $\eta = 1$, the contribution of mock gravity can be comparable to gravity only at $z > 100$ without violating the constraints. Let us now explore the configurations that would result if mock gravity was dominant.

If we ignore all forces but those contributed by mock gravity and by gas pressure (of course we have no idea what the external pressure would be at such high z), we find the following solutions:

$$W_{\rm eq} = 0.68\ {\rm kpc} \left(\frac{u}{10^4 u_0}\right)^{-1} \left(\frac{g_D}{0.01}\right)^{-2} \left(\frac{T}{10{,}000\ {\rm K}}\right) \times \left(\frac{N_{\rm tot}}{9.0 \times 10^{21}\ {\rm cm}^{-2}}\right)^{-1} \tag{29a}$$

$$n_{\rm tot} = 4.3\ {\rm cm}^{-3} \left(\frac{u}{10^4 u_0}\right) \left(\frac{g_D}{0.01}\right)^2 \left(\frac{T}{10{,}000\ {\rm K}}\right)^{-1} \times \left(\frac{N_{\rm tot}}{9.0 \times 10^{21}\ {\rm cm}^{-2}}\right)^2 \tag{29b}$$

$$\tau_{\mathrm{Ly}\alpha} = 0.8\left(\frac{g_D}{0.01}\right)^2\left(\frac{T}{10{,}000\ \mathrm{K}}\right)^{-2.25}\left(\frac{E_\gamma}{13.6\ \mathrm{eV}}\right)^4 \times \left(\frac{N_{\mathrm{tot}}}{9.0\times10^{21}\ \mathrm{cm}^{-2}}\right)^3 \quad (29c)$$

$$N_{\mathrm{H}}/N_{\mathrm{tot}} = 1.1\times10^{-9}\left(\frac{g_D}{0.01}\right)^2\left(\frac{T}{10{,}000\ \mathrm{K}}\right)^{-1.75} \times \left(\frac{E_\gamma}{13.6\ \mathrm{eV}}\right)^4\left(\frac{N_{\mathrm{tot}}}{9.0\times10^{21}\ \mathrm{cm}^{-2}}\right)^2 . \quad (29d)$$

(We have written this solution in terms of the value of u that yields equal contributions from mock gravity and gravity for $g_D = 0.01$.) Mock gravity will yield an equilibrium at a higher density, a smaller neutral fraction, and a smaller width, than will ordinary gravity alone. If this slab has density exceeding the mean baryonic density at a given z, then mock gravity on dust may have enhanced structure formation. The width a slab with total column N_{tot} would occupy at density $n_{\mathrm{baryon}} = \Omega_b n_{\mathrm{crit}}$ is given by $W_{\mathrm{crit}} = 9.8\times10^6$ kpc $(1+z)^{-3}$ $(N_{\mathrm{tot}}/9.0\times10^{21}\ \mathrm{cm}^{-2})(\Omega_b h^2/0.025)^{-1}$. The condition $W_{\mathrm{eq}} = W_{\mathrm{crit}}$ yields

$$N_{\mathrm{lim}} = 2.7\times10^{21}\ \mathrm{cm}^{-2}\left(\frac{T}{10{,}000\ \mathrm{K}}\right)^{1/2} \times\left[\frac{u(1+z)^{-4}}{8\times10^{-5}u_0}\right]^{-1/2}\left(\frac{g_D}{0.01}\right)^{-1} \times\left(\frac{\Omega_b h^2}{0.025}\right)^{1/2}\left(\frac{1+z}{100}\right)^{-1/2}, \quad (30)$$

the limiting column density above which structure will grow. (Here we express the radiation density in terms of the FIRAS limit.) Although the long dimension of the slab exceeds W_{eq} by an unknown factor, we can express N_{lim} as $7\times10^8\ M_\odot/W_{\mathrm{eq}}^2$ which provides a lower limit to the mass above which structure will grow. This total column density corresponds to

$$N_{\mathrm{H}} > 2.7\times10^{11}\ \mathrm{cm}^{-2}\left(\frac{T}{10{,}000\ \mathrm{K}}\right)^{-1/4} \times\left(\frac{E_\gamma}{13.6\ \mathrm{eV}}\right)^4\left[\frac{u(1+z)^{-4}}{8\times10^{-5}u_0}\right]^{-3/2} \times\left(\frac{g_D}{0.01}\right)^{-1}\left(\frac{\Omega_b h^2}{0.025}\right)^{3/2}\left(\frac{1+z}{100}\right)^{-3/2} . \quad (31)$$

At higher z, this limiting column density is smaller, meaning that smaller structures could form earlier and grow if there was an adequate radiation field and dust. If E_γ is increased, the same low N_{H} structure would not begin to separate from the Hubble flow as soon (although the smallest neutral column density object to form at z would have the same N_{tot} independent of E_γ).

As the simplest example, let us assume that the radiation is produced as a sudden burst with a spectrum that is a δ-function in E_γ. Then, from § 2.1, $u \propto J_\nu \propto (1+z)^4$, and we assume $T \propto E_\gamma^{1/3} \propto (1+z)^{1/3}$. As long as the radiation is not shifted below the ionization threshold (and still assuming that the external pressure has negligible influence) a slab with a given N_{tot} evolves as

$$W_{\mathrm{eq}} \propto (1+z)^{-3.7} , \quad (32a)$$

$$N_{\mathrm{H}}/N_{\mathrm{tot}} \propto (1+z)^{3.4} . \quad (32b)$$

It becomes more ionized and thicker with decreasing z, due to the energy redshifting toward the ionization threshold. This behavior continues until one of three thngs happens: (1) $E_\gamma <$ 13.6 eV, (2) radiation is absorbed by dust, (3) gravity dominates mock gravity $[(u/u_0)g_D^2 < 1]$.

Starting from critical density, the time scale to reach equilibrium for a given N_{tot} is an important quantity. Suppose, for example, we start with a density fluctuation that is twice the mean baryonic density (corresponding to a scale of $W_{\mathrm{crit}}/2$) and consider how long compression to equilibrium will take. The compressing force is that of mock gravity so the time scale is given by

$$t_{\mathrm{collapse}} \sim (W_{\mathrm{crit}} N_{\mathrm{tot}} m_{\mathrm{H}}/4F_{\mathrm{mock}})^{1/2} \quad (33)$$

for $W_{\mathrm{eq}} \ll W_{\mathrm{crit}}$. Using (20a), we obtain

$$t_{\mathrm{collapse}} \sim 1.7\times10^{11}\ \mathrm{yr}\left(\frac{u}{u_0}g_D^2\right)^{-1/2}(1+z)^{-3/2}\left(\frac{\Omega_b h^2}{0.025}\right)^{-1/2} . \quad (34)$$

For comparison the Hubble time is

$$t_{\mathrm{H}} \sim 1.5\times10^{10}\ \mathrm{yr}\ (1+z)^{-3/2} , \quad (35)$$

yielding a ratio

$$t_{\mathrm{collapse}}/t_{\mathrm{H}} \sim 11.3\left(\frac{u}{u_0}g_D^2\right)^{-1/2} \quad (36)$$

which is independent of N_{tot} and z. The time scale for structure growth via mock gravity is too long unless $(u/u_0)g_D^2 \gg 1$, or unless we begin with a larger seed density that arose by other means.

The above scenario also requires star formation at high z in order to make dust. We have used the modest value of 1% of the galactic dust abundance in our estimates above. A similar value was suggested by Peebles (private communication 1991), in a model intended to smooth out fluctuations in the microwave background through absorption by dust grains at $z \sim 100$. Although the existence of such dust is dubious, we should note that the stars required to produce the dust will naturally create the ionizing radiation that is needed for mock gravity. This is obtained by assuming that for each solar mass of metals, $10^{-3}\ M_\odot\ c^2$ of energy is emitted in the UV. A dust abundance 1% of galactic thus leads to an energy density per steradian of $\sim 5.3\times10^{-4}\ (1+z)^3 u_0$. This is smaller than the *COBE* FIRAS limit of $\sim 8\times10^{-5}\ (1+z)^4 u_0$ at very high z and is large enough to lead to a significant mock gravity force at $z > 100$ on mass scales larger than $\sim 10^9\ M_\odot$.

It is difficult to be more specific due to the many uncertainties in the set-up parameters. The numbers given in this section indicate that models with a dominant mock gravity force and a short enough time scale for structure formation are rather close to violating current FIRAS constraints. Ways of avoiding this problem include adding more dust to the models, pushing the mechanism to higher z, and hiding radiation in a less rigorously constrained spectral regime. There can also be a mock gravity effect in particular environments, where larger radiation fields and excess dust are present, without violating overall constraints. We conclude that this highly speculative model in which mock gravity on dust may influence structure formation on small scales is unlikely, but is not ruled out.

5. MODELS FOR LYMAN ALPHA CLOUDS

In § 3, we presented a very general expression for the equilibrium state of the slabs. In §§ 3.2 and 4 we discussed the

circumstances in which Lyα trapping and mock gravity could be important. Now we shall focus on the era from approximately redshift 5 until the present, and on slabs with a uniform incident extragalactic background. Under these conditions, the equilibrium is a balance of external pressure, gravity, and gas pressure.

5.1. *General Equilibrium Solutions*

The balance of forces in this simple case is given by the equation

$$\frac{\pi}{4} G m_{\rm H}^2 N_{\rm tot}^2 \eta + P_{\rm ext} = 2 n_{\rm tot} kT \, . \tag{37}$$

The external pressure, $P_{\rm ext}$, is related to the density $\Omega_{\rm ext}$ and temperature $T_{\rm ext}$ of the external medium by equation (6). The parameter η is defined as

$$\eta(N_{\rm tot}) = 1 + \frac{\rho_{\rm DM}}{\rho_{\rm gas}} , \tag{38}$$

where $\rho_{\rm DM}$ and $\rho_{\rm gas}$ are densities of dark matter and gas which we assume have a constant ratio within the gaseous slab, so that η is a function only of $N_{\rm tot}$. It is convenient to define a constant N_1, the value of $N_{\rm tot}$ for which the forces contributed by gravity and by external pressure are equal. We denote the values of $n_{\rm tot}$, η, and W at $N_{\rm tot} = N_1$ by n_1, η_1, and W_1:

$$N_1 = \left(\frac{4k}{\pi G m_{\rm H}^2 \eta_1}\right)^{1/2} \left(\frac{P_{\rm ext}}{k}\right)^{1/2}$$

$$= 3.1 \times 10^{19} \eta_1^{-1/2} \left(\frac{P_{\rm ext}}{k}\right)^{1/2} \ {\rm cm}^{-2} , \tag{39a}$$

$$n_1 = P_{\rm ext}/2kT , \tag{39b}$$

$$W_1 = N_1/n_1 . \tag{39c}$$

Equations (7) and (39) then give the density and degree of ionization as a function of η/η_1 and $N_{\rm tot}/N_1$,

$$\frac{n_{\rm tot}}{n_1} = \left[\left(\frac{N_{\rm tot}}{N_1}\right)^2 \left(\frac{\eta}{\eta_1}\right) + 1\right] , \tag{40a}$$

$$\frac{N_{\rm H}}{N_{\rm tot}} = \frac{\alpha_{\rm rec} n_1}{\zeta} \left[\left(\frac{N_{\rm tot}}{N_1}\right)^2 \left(\frac{\eta}{\eta_1}\right) + 1\right] . \tag{40b}$$

For monochromatic photons the ionization rate in equation (3) can be written as

$$\zeta = 1.6 \times 10^{-7} \left(\frac{u}{u_0}\right) \left(\frac{E_\gamma}{13.6 \ {\rm eV}}\right)^{-4} \ {\rm s}^{-1} \tag{41}$$

In general, η depends on $P_{\rm ext}$ and $N_{\rm tot}$. Instead of considering explicit models of the dark matter distribution we parameterize our ignorance by assuming

$$\rho_{\rm DM} \propto N_{\rm tot}^{\gamma} , \tag{42}$$

independent of $P_{\rm ext}$. Plausible examples are bracketed by two cases: (1) $\gamma = 0$, constant density spherical halos, where $N_{\rm DM}$, the total column density of dark matter, and $N_{\rm tot}$ scale like the radius; and (2) $\gamma = 1.5$, spherical halos in which the dark matter mass and gas mass are independent of the radius, i.e., the same total mass surrounding all slabs. Recalling the definitions of η_1 and N_1 from equation (39a), we can write

$$\eta(N_{\rm tot}) = 1 + (\eta_1 - 1) \left(\frac{N_{\rm tot}}{N_1}\right)^{\gamma} \left(\frac{2F_{\rm ext}}{F_{\rm gas}}\right) , \tag{43}$$

and for $\eta \gg 1$ and $N_{\rm tot} \gg N_1$, using equation (40a) this reduces to

$$\eta(N_{\rm tot}) = \eta_1 \left(\frac{N_{\rm tot}}{N_1}\right)^{(\gamma/2)-1} . \tag{44}$$

Thus η is constant for the unlikely case with $\gamma = 2$.

For $N_{\rm tot}/N_1$ very small, the square bracket in equation (40) reduces to unity. For $N_{\rm tot}/N_1$ so large that $\eta_1 \gg 1$ and $\eta \gg 1$ (dark matter dominant) the limiting solution is

$$\frac{n_{\rm tot}}{n_1} = \left(\frac{N_{\rm tot}}{N_1}\right)^{\gamma/2+1} , \tag{45a}$$

$$\frac{N_{\rm H}}{N_{\rm tot}} = \frac{\alpha_{\rm rec} n_1}{\zeta} \left(\frac{N_{\rm tot}}{N_1}\right)^{(\gamma/2)+1} . \tag{45b}$$

Throughout this paper, we will consider the temperature as a free parameter, using $T = 10{,}000$ K in numerical examples. Given the properties of incident radiation and the total gas density, we can estimate the equilibrium temperature by a balance of heating and cooling. The equilibrium temperature can be obtained by solution of the equations of charge conservation, ionization/recombination balance for H and He, and the condition of thermal equilibrium (as in Black [1981] for spherical clouds). If most photons are below 40 eV or if metals are present, temperatures in the range 10,000–30,000 K result. Clouds significantly colder would imply either nonequilibrium expansion (Duncan, Vishniac, & Ostriker 1991), or very dense neutral slabs (Donahue & Shull 1991).

5.2. *Transitions between Regimes*

We are interested in the relationship between the column density distribution $g(N_{\rm tot})$ for clouds considering all hydrogen (ionized and neutral), and $f(N_{\rm H})$, the column density distribution for neutral H alone. (Due to random orientation of slabs the observed column density has a mean value of twice the perpendicular value. When comparing with observations throughout we will apply this correction to the theoretical models.) The number of clouds is unique so we have $g(N_{\rm tot}) dN_{\rm tot} = f(N_{\rm H}) dN_{\rm H}$. Since observations suggest a power-law distribution for $f(N_{\rm H})$, at least over a small range of $N_{\rm H}$, we shall assume a power law for $g(N_{\rm tot})$,

$$g(N_{\rm tot}) = C_t N_{\rm tot}^{-\epsilon} , \tag{46}$$

over a fairly large range between limiting column densities $N_{\rm min}$ and $N_{\rm max}$. The contribution of all clouds to Ω in terms of the intergrated column density $N_{\rm int}$ is then

$$\Omega_{\rm cl} = \frac{m_{\rm H} H_0}{\rho_{\rm crit} c} N_{\rm int} , \tag{47a}$$

$$N_{\rm int} = \int_{N_{\rm min}}^{N_{\rm max}} g(N_{\rm tot}) N_{\rm tot} \, dN_{\rm tot} . \tag{47b}$$

Depending on the value of ϵ we have

$$N_{\rm int} = \frac{C_t}{\epsilon - 2} N_{\rm min}^{2-\epsilon} , \qquad \epsilon > 2 , \tag{48a}$$

$$N_{\rm int} = \frac{C_t}{2 - \epsilon} N_{\rm max}^{2-\epsilon} , \qquad \epsilon < 2 , \tag{48b}$$

$$N_{\rm int} = C_t \ln(N_{\rm max}/N_{\rm min}) , \quad \epsilon = 2 . \tag{48c}$$

If the range of validity of equation (46) is large enough, there will be three different regimes within this range. Well inside

each of the three regimes, the relation between N_H and N_{tot} also leads to a power-law form for the neutral column density spectrum:

$$f(N_H) = C_H N_H^{-\beta} . \quad (49)$$

Then the value of β can be determined in the three regimes: (1) For $N_{min} < N_{tot} \ll N_1$ (in the pressure-dominated regime) we have

$$\beta = \epsilon \quad (50a)$$

$$C_H = C_t \left(\frac{\alpha_{rec} n_1}{\zeta} \right)^{\epsilon - 1} . \quad (50b)$$

(2) In the gravity-dominated regime, we can use equation (45b). This gives

$$\beta = \frac{\epsilon + (\gamma/2) + 1}{(\gamma/2) + 2} , \quad (51a)$$

$$C_H = \frac{C_t}{(\gamma/2) + 2} \left(\frac{\alpha_{rec} n_1}{\zeta} \right)^{(\epsilon - 1)/[(\gamma/2) + 2]} \times N_1^{\{(1 - \epsilon)[(\gamma/2) + 1]/[(\gamma/2) + 2]\}} . \quad (51b)$$

We shall see that values $1.5 \lesssim \epsilon \lesssim 2$ are most likely. With $0 < \gamma < 1.5$, equation (51a) always gives $\beta < \epsilon$. (3) When N_{tot} is so enormous that most photons are destroyed in the outermost layers of the slab we have $N_H \sim N_{tot}$, $\beta = \epsilon$, and $C_H = C_t$. The three regimes are illustrated schematically in Figure 1.

In the two transition regions between the three regimes the relationship between $g(N_{tot})$ and $f(N_H)$ is more complicated, especially in the "recombination region" between (2) and (3). The effects of this transition and lack of observational evidence were first discussed by Tytler (1987). Up until now, we have not needed to consider the form of the spectrum, because the equilibrium solution only depended upon ζ. However, this transition depends on the energy of the ionizing radiation.

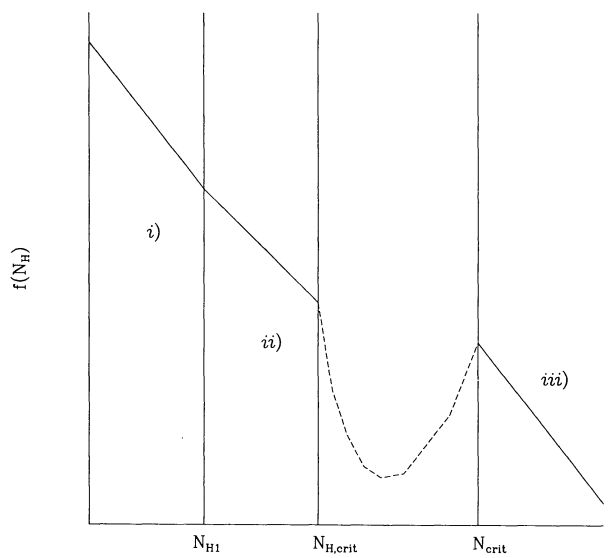

FIG. 1.—A schematic illustration of the three regimes of behavior for the distribution of neutral column densities. Regime 1 is the pressure-dominated regime, where the slope is equal to ϵ (eq. [50a]). In regime 2 gravity dominates the inward force and eq. (51a) gives the slope. Regime 2 is the optically thick regime where $N_H = N_{tot}$. The shape of the transition between regimes 2 and 3 is approximate and will depend on the details of the spectrum.

Consider first the hypothetical case of monochromatic photons of energy (13.6R)eV, which require an H I column density of $N_{H,crit} = 1.6 \times 10^{17} R^3$ for unit optical depth. Equations (40) and (45b) allow determination of the corresponding critical value N_{crit} of the total column density as

$$N_{crit} = \frac{\zeta}{\alpha_{rec} n_1} N_{H,crit} , \quad N_{crit} < N_1 , \quad (52a)$$

$$N_{crit} = \left(\frac{\zeta}{\alpha_{rec} n_1} \right)^{1/(\gamma/2 + 2)} N_1^{(\gamma/2 + 1)/(\gamma/2 + 2)} \times N_{H,crit}^{1/(\gamma/2 + 2)} , \quad N_{crit} > N_1 , \quad (52b)$$

in the pressure- and gravity-dominated regimes. As long as $N_1 < N_{crit}$, we have $N_{crit} \gg N_{H,crit}$, thus an interesting feature of this transition for monochromatic photons is the prediction of a gap (and not merely a break) in $f(N_H)$. As in Strömgren sphere theory, N_H increases rapidly from $\sim N_{H,crit}$ to $\sim N_{crit} \gg N_{H,crit}$ as N_{tot} varies only from $\sim N_{crit}$ to $\sim 2N_{crit}$. Because $d \ln N_H / d \ln N_{tot}$ is so large in the transition region, the distribution $f(N_H)$ should be extremely small there. This temporary drop in $f(N_H)$ is shown only schematically in Figure 1 and has not been calculated here. The sharpness of the drop depends not only on $N_{crit}/N_{H,crit}$ (discussed above), but also on the shape of the photon spectrum. If the spectrum were very flat (large range of R) the initial drop would be less sharp (see the parameter y' in Corbelli & Salpeter; 1992).

5.3. *Specific Examples*

Now we will consider some particular examples, emphasizing the locations of the transitions discussed above. In the following sections we consider the model predictions for $f(N_H)$ and cloud evolution, for these same examples. The value of N_1 is set once P_{ext} and η_1 are given. Cases A–C explore the consequences of choosing different values of P_{ext} which yield N_1 within, above, and below the Lyα forest cloud regime. It is most useful to express these examples in terms of the neutral column density N_{H1} at which the transition between external pressure and gravity domination is expected to occur. The relationship between external pressure and N_{H1} is

$$P_{ext}/k = 1 \text{ cm}^{-3} \text{ K} \left(\frac{T}{10{,}000 \text{ K}} \right)^{7/6} \left(\frac{\zeta}{2.7 \times 10^{-12} \text{ s}^{-1}} \right)^{2/3} \times \left(\frac{\eta_1}{10} \right)^{1/3} \left(\frac{N_{H1}}{1.4 \times 10^{14} \text{ cm}^{-2}} \right)^{2/3} , \quad (53)$$

where the ionization rate ζ is expressed in terms of the value given by the proximity effect ($\zeta = 2.7 \times 10^{-12} \text{ s}^{-1}$).

The results are qualitatively similar as long as $N_{H,min} < N_{H1} \ll N_{H,crit}$. However, in some ranges of N_H our choice of ϵ depends on the value of N_{H1} (and on which observational power law is finally verified). We start with case A, appropriate if the suggestion by Jenkins, Bajtlik, & Dobrzycki (1992) of a double power law $f(N_H)$ should be verified.

5.3.1. Case A: $N_{H,min} \ll N_{H1} = 1.5 \times 10^{13}$, $\epsilon = 2.0$

Equation (50a) gives $\beta = \epsilon = 2.0$ for $N_H \ll 1.5 \times 10^{13}$, which agrees with equation (4) for small N_H. (N_H, in our equations, is defined as the normal column density including both half-slabs. Because of random orientations of slabs, this corresponds to approximately half the observed values.) Various

quantities at the transition between the two regimes are

$$N_1 = 2.0 \times 10^{19}\ \mathrm{cm}^{-2}\ \eta_1^{-1/3}\left(\frac{T}{10{,}000\ \mathrm{K}}\right)^{7/12} \times \left(\frac{\zeta}{2.7 \times 10^{-12}\ \mathrm{s}^{-1}}\right)^{1/3}, \quad (54a)$$

$$P_{\mathrm{ext}}/k = 0.11\ \mathrm{cm}^{-3}\ \mathrm{K}\ \eta_1^{1/3}\left(\frac{T}{10{,}000\ \mathrm{K}}\right)^{7/6} \times \left(\frac{\zeta}{2.7 \times 10^{-12}\ \mathrm{s}^{-1}}\right)^{2/3}, \quad (54b)$$

$$n_1 = 5.3 \times 10^{-6}\ \mathrm{cm}^{-3}\ \eta_1^{1/3}\left(\frac{T}{10{,}000\ \mathrm{K}}\right)^{1/6} \times \left(\frac{\zeta}{2.7 \times 10^{-12}\ \mathrm{s}^{-1}}\right)^{2/3}. \quad (54c)$$

This value of P_{ext} corresponds to

$$\Omega_{\mathrm{ext}}\, T_{\mathrm{ext}} = 3.7 \times 10^2\left(\frac{1+z}{3.5}\right)^{-3}\eta_1^{1/3} \quad (55)$$

for our standard adopted values of ζ and T, i.e., setting the quantities in parenthesis equal to one.

First, we shall concentrate on the case with no dark matter ($\eta = \eta_1 = 1$). Then the equilibrium can be written as

$$n = 5.3 \times 10^{-6}\ \mathrm{cm}^{-3}\left[\left(\frac{N_{\mathrm{tot}}}{N_1}\right)^2 + 1\right], \quad (56a)$$

$$W_{\mathrm{eq}} = 1.2 \times 10^3\ \mathrm{kpc}\ \frac{(N_{\mathrm{tot}}/N_1)}{[(N_{\mathrm{tot}}/N_1)^2 + 1]}, \quad (56b)$$

$$N_{\mathrm{H}} = 8.0 \times 10^{12}\ \mathrm{cm}^{-2}\left[\left(\frac{N_{\mathrm{tot}}}{N_1}\right)^3 + \left(\frac{N_{\mathrm{tot}}}{N_1}\right)\right], \quad (56c)$$

$$\tau_{\mathrm{Ly}\alpha} = 0.64\left[\left(\frac{N_{\mathrm{tot}}}{N_1}\right)^3 + \left(\frac{N_{\mathrm{tot}}}{N_1}\right)\right], \quad (56d)$$

$$N_{\mathrm{H}}/N_{\mathrm{tot}} = 1.0 \times 10^{-6}\left[\left(\frac{N_{\mathrm{tot}}}{N_1}\right)^2 + 1\right]. \quad (56e)$$

Since we have set the value of ϵ to correspond to $f(N_H)$ in the pressure-dominated regime of Jenkins, Batjlik, & Dobrzycki (1992), equation (56e) allows us to predict the value of β in the gravity-dominated regime. The result for the case with no dark matter is $\beta = 1.33$. This is quite consistent with the exponent suggested in equation (4), $\beta = 1.3$.

The solutions in equation (56) are illustrated in Figures 2 *a–d*. The solid lines refer to cases without dark matter. Figure 2 also gives curves for a model with dark matter of the form and quantity $\gamma = 1$ and $\eta_1 = 10$. With the addition of dark matter, for a fixed N_{H}, less total gas is required to balance the gas pressure, thus the equilibrium is at a higher neutral fraction and a smaller width. The large slab widths seen in Figure 2*b* for values near N_{H1} are of concern, since they may violate the assumption of equilibrium. Additional dark matter can alleviate this problem. Dark matter also changes the value of β in regime (3) (gravity-dominated regime) as described in equation (51). For $\gamma = 0$ we have $\beta = 1.5$, while $\gamma = 1$ (the example in the figures) would yield $\beta = 1.4$.

Equation (56) only applies below the transition to the optically thick regime. Figure 2 also illustrates the transition from region (2) to region (3) for δ-functions at energies 13.6, 25, and 60 eV. If $J(\nu) \propto \nu^{-1.5}$ applies down to 13.6 eV, the typical photon energy is 25 eV, but the break is not as sharp as for monochromatic photons. If photons very close to 13.6 eV are important, the gap in $f(N_{\mathrm{H}})$ should occur just in the region where the Lyman limit observations are most detailed for intermediate and large z. Therefore, the absence of an observed break corroborates Madau's suggestion that photons between 13.6 eV and roughly twice this value are attenuated by other Lyα clouds. (As seen in Figure 2*a*, adding dark matter to a slab in a monochromatic 13.6 eV background will decrease slightly the width of the gap, but will not alter its starting point in N_{H}.) For $E_\gamma = 25$ eV, equation (52b) yields $N_{\mathrm{crit}} = 7.5 \times 10^{20}\ \mathrm{cm}^{-2}$. The neutral column density increases from $N_{\mathrm{H,crit}} = 10^{18}\ \mathrm{cm}^{-2}$ to $\sim N_{\mathrm{crit}}$ as N_{tot} varies from N_{crit} to $\sim 2N_{\mathrm{crit}}$.

Using equations (47) and (48c), we can compute the contribution of the family of clouds to Ω for this model with $\epsilon = 2$. The result of intergrating over three orders of magnitude in N_{tot} (i.e., $N_{\mathrm{max}}/N_{\mathrm{min}} = 10^3$) is $\Omega_{\mathrm{cl}} = 0.006\eta_1^{1/3}h$. This, roughly speaking, includes contributions from all clouds with N_{H} in the range 10^{12}–$10^{18}\ \mathrm{cm}^{-2}$. There will be an additional, and comparable, contribution from the damped Lyα systems in regime (3).

It is also possible that the external pressure is very low. Then we have a variation on case A, which we will denote case A′, where $N_{\mathrm{H1}} \ll 10^{13}\ \mathrm{cm}^{-2}$. In this case we must turn to confinement by gravity for slabs of all column densities. We will not present a specific example of this case, but there are a few relevant comments. If $P_{\mathrm{ext}}/k \lesssim 0.03\ \mathrm{cm}^{-3}\ \mathrm{K}$ ($\Omega_{\mathrm{ext}}\, T_{\mathrm{ext}} \lesssim 100$ at $z \sim 2.5$), the transition should still appear somewhere below $N_{\mathrm{H}} = 10^{13}$ in future data. However, it is also possible that there is a break in $g(N_{\mathrm{tot}})$ for these lower mass slabs. Thus the cloud mass spectrum may fall to zero before such a transition is evidenced. As compared to case A, the equilibrium slabs at small N_{H} will have lower density, larger width, and smaller neutral fractions. The large width could be a problem for these models, although as noted for the previous case, dark matter can help.

5.3.2. Case B: $N_{\mathrm{H,min}} \sim 10^{12}\ \mathrm{cm}^{-2}$, $N_{\mathrm{H1}} \sim 10^{16}\ \mathrm{cm}^{-2}$, $\epsilon = 1.6$

This is an example which would be appropriate if observations should verify $\beta \sim 1.6$ for $\log N_{\mathrm{H}} \sim 13$–14, but a slower increase below $\log N_{\mathrm{H}} = 13$. As we showed in § 5.2, a break with this shape could not result from the transition from pressure to gravity domination. It must then be a signature of a decrease in ϵ at small N_{H}.

The external pressure is set at a much larger value than in case A so that the transition from regime (1) to regime (2) occurs just below the Lyman limit. The normalizations at the transition at $N_{\mathrm{H1}} = 10^{16}\ \mathrm{cm}^{-2}$ take the same form as equation (54), but with coefficients $1.7 \times 10^{20}\ \mathrm{cm}^{-2}$ for N_1, $8.0\ \mathrm{cm}^{-3}\ \mathrm{K}$ for P_{ext}/k, and $3.9 \times 10^{-4}\ \mathrm{cm}^{-3}$ for n_1. Without dark matter (below the transition region to the optically thick regime) the coefficients for case A in equation (56) in this case become $3.9 \times 10^{-4}\ \mathrm{cm}^{-3}$, 141 kpc, $5.0 \times 10^{15}\ \mathrm{cm}^{-2}$, and 400 for n, W_{eq}, N_H, and τ_{Lya}, respectively. The neutral and total column densities are related by

$$N_{\mathrm{H}}/N_{\mathrm{tot}} = 2.9 \times 10^{-5}\left[\left(\frac{N_{\mathrm{tot}}}{N_1}\right)^2 + 1\right]. \quad (57)$$

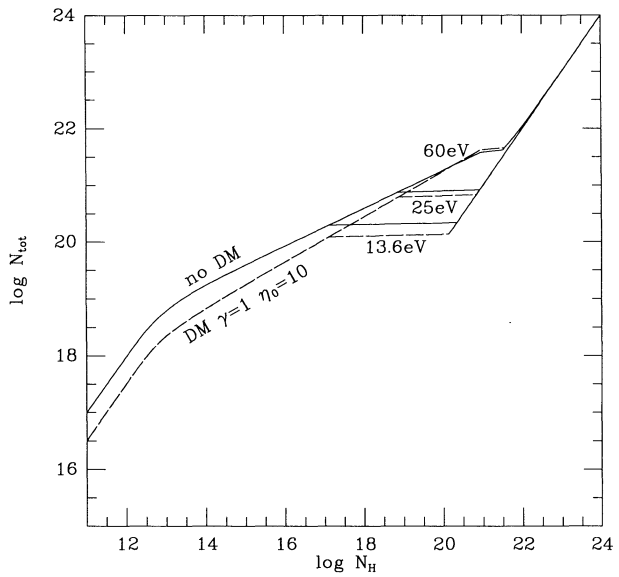

FIG. 2a

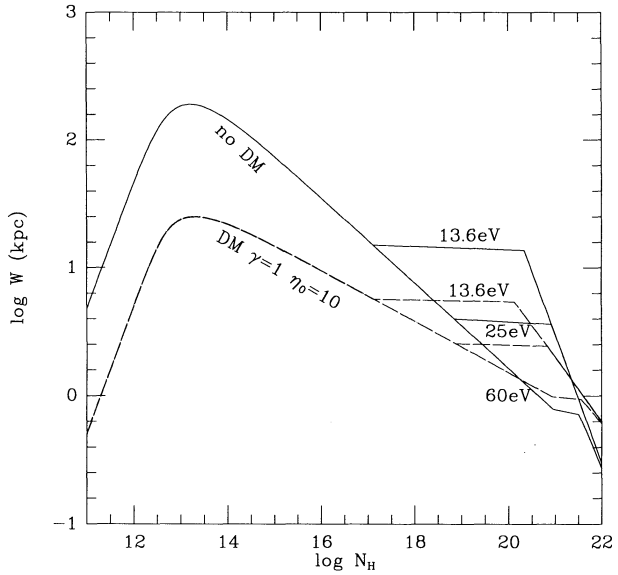

FIG. 2b

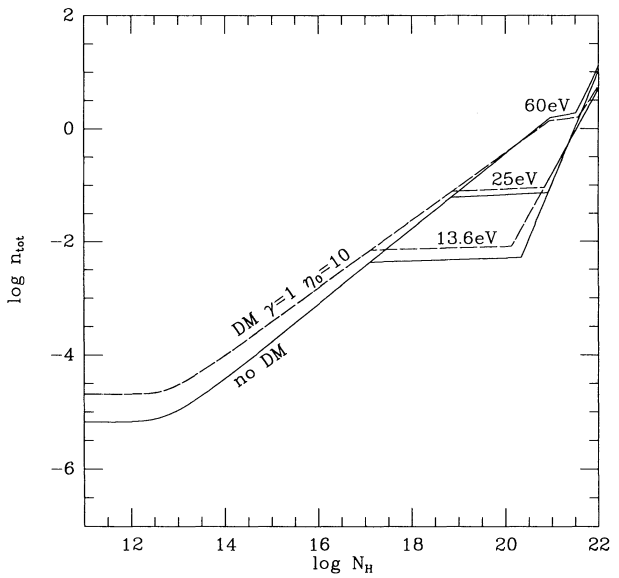

FIG. 2c

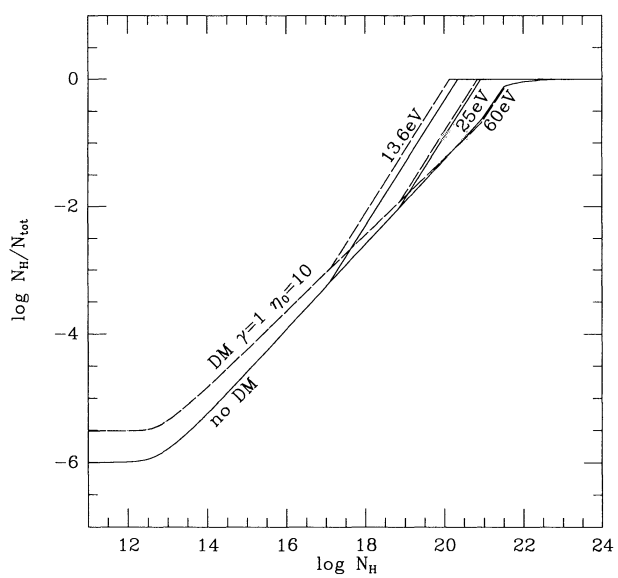

FIG. 2d

FIG. 2.—Dependence of various slab equilibrium quantities on the neutral column density, N_H, for the example (case A) with the transition from pressure to gravity domination at $N_{H1} = 1.5 \times 10^{13}$ cm^{-2}. Solid curves depict the case with no dark matter, while dotted lines represent an example including dark matter with $\eta_1 = 10$ and $\gamma = 1$. The transition from the optically thin to the optically thick regime is illustrated schematically for a δ-function spectrum of incident radiation with three different energies. The vertical axes display: (*a*) the total column density of neutral and ionized H in cm^{-2}, (*b*) the slab equilibrium width in kpc, (*c*) the total number density of H in cm^{-3}, and (*d*) the neutral fraction.

These solutions are illustrated in Figure 3, for the same parameters (ζ, T, η_1, γ) as for case A in Figure 2. As the external pressure is increased, we have a larger region of pressure domination. Within this region, the slab tends to be less ionized than if the confinement were due to gravity. The equilibrium for a given N_H is a thinner slab, with a larger density. This slab will have $N_{crit} = 4.9 \times 10^{20}$ cm^{-2} for $N_{H,crit} = 10^{18}$ cm^{-2}, a larger neutral fraction than in case A.

In this example we have chosen N_{H1} in a region where N_H measurements are not accurate. Equation (51a) definitely predicts a smaller β at the low end of the Lyman limit range (10^{16}–10^{18} cm^{-2}) than either above or below this range. Using equations (47) and (48b) (and the normalization determined in § 5.4) we find $\Omega_{cl} = 1.2 \times 10^{-11}\ N_{max}^{0.5}$, which yields $\Omega_{cl} = 7.5 \times 10^{-3}\ h$ for $N_{max} = 10^{22}$ cm^{-2}.

5.3.3. Case B′: $N_{H,min} \sim 10^{12}$ cm^{-2}, $N_{H1} = 10^{16}$ cm^{-2}, $\epsilon = 2$

The relationship between N_{tot} and N_H does not depend upon ϵ, thus Figure 3 will apply to this case as well. Changing ϵ does, however, impact the distribution of N_H predicted by a model, thus we will need to consider this case separately in the following subsection. The choice of $\epsilon = 2$ means that equation (48c)

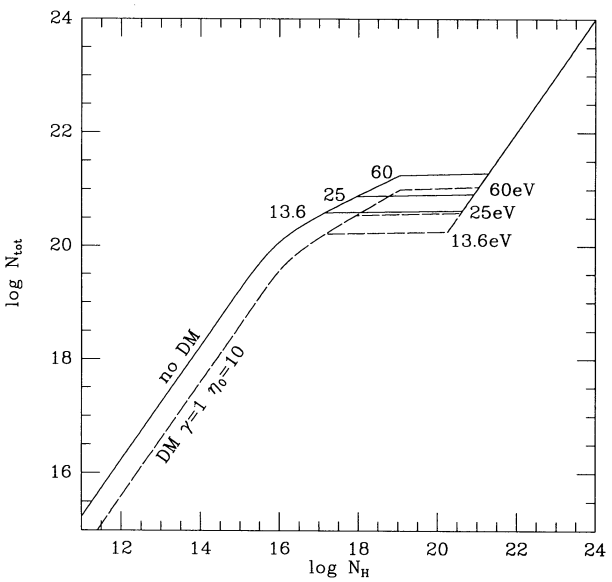

FIG. 3a

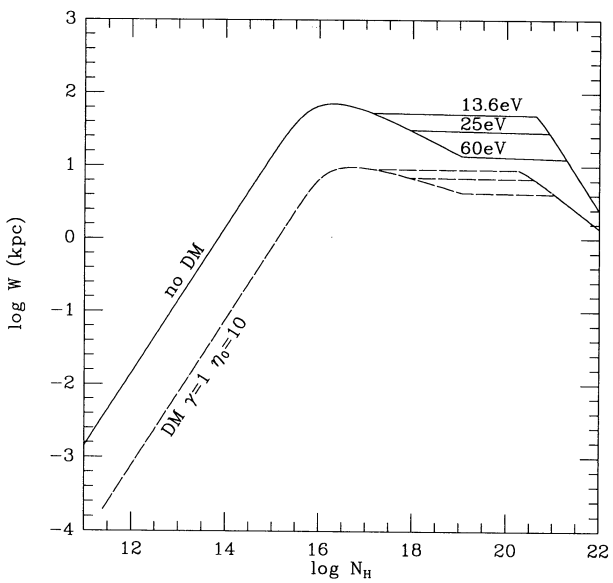

FIG. 3b

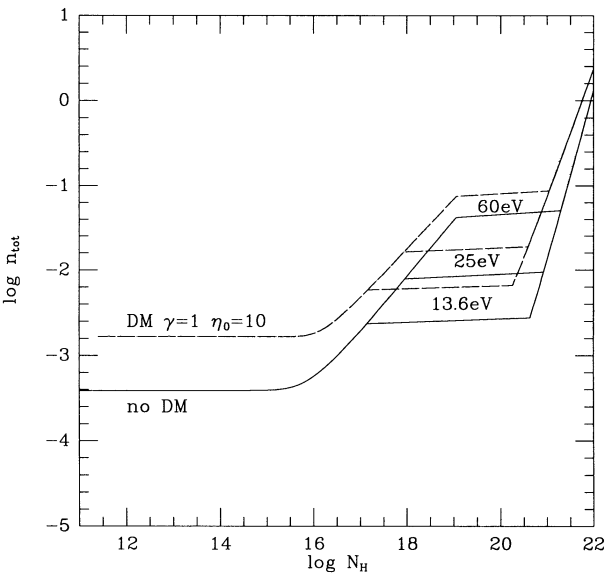

FIG. 3c

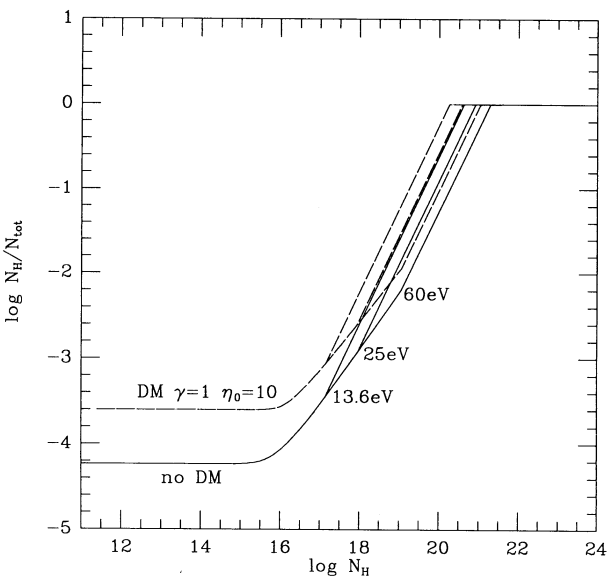

FIG. 3d

FIG. 3.—Same as Fig. 2, but with the transition from pressure to gravity domination at $N_{H1} = 10^{16}$ cm^{-2} (case B).

will apply, as in case A, but a different normalization leads to smaller contribution of $\Omega_{cl} = 5.0 \times 10^{-4}\ h$ for $N_{max}/N_{min} = 10^6$ (e.g., for the range 10^{12} cm$^{-2} < N_H < 10^{22}$ cm^{-2}).

5.3.4. $N_{H,min} \ll N_{H1}$, $N_{H1} = 10^{18}$ cm^{-2}, $\epsilon = 1.6$

If, observationally, β never gets below 1.5 in the Lyα forest region, we may have to choose N_{H1} near 3×10^{17} cm^{-2} or above. This requires $P_{ext}/k \gtrsim 1.6 \times 10^2$ cm^{-3} K for $\eta_1 = 10$. The "gap" in the $f(N_H)$ distribution that results from the transition to the optically thick regime leads to a very large β in this transition range. However, in this case β is decreased above N_{H1} due to the pressure to gravity-domination transition. If these two effects coincide, this case may fortuitously mimic constant β. We have chosen to consider here the particular case with a transition from pressure to gravity domination safely within the Lyman limit regime, so that at $z = 2.5$ all of the Lyα forest clouds are pressure confined. The transition value $N_{H1} = 10^{18}$ cm^{-2} is obtained from $P_{ext}/k = 366$ cm^{-3} K for our standard choices of $\zeta = 2.7 \times 10^{-12}$ s^{-1} and $\eta_1 = 10$. This value of P_{ext}/k is slightly smaller than the *COBE* y-parameter limit. We will show in § 5.4 that this pressure is suggested by the relative level of damped Lyα and Lyα forest clouds. For this choice of parameters $N_1 = 1.9 \times 10^{20}$ cm^{-2}, $n_1 = 0.018$ cm^{-3}, $W_1 = 3.4$ kpc. The slab density will be constant at n_1 and the neutral fraction $N_H/N_{tot} = 2.8 \times 10^{-3}$ for $N_H < N_{H1}$. Since the transition to the optically thick regime begins at $N_{H,crit} = N_{H1}$ for $E\gamma = 25$ eV, we have $N_{crit} = N_1 = 1.9 \times 10^{20}$ cm^{-2}. Gravity and external pressuere are equal at this transition. The contribution to Ω for clouds with log $N_H < 10^{22}$ is $\Omega_{cl} = 1.2 \times 10^{-3}\ h$ (see eqs. [47] and [48b], and

§ 5.4 for normalization), with only a small contribution from the forest ($\Omega_{cl} = 9.8 \times 10^{-5}\, h$ for $\log N_H < 10^{17}$).

5.4. *Comparison of Models with the Observed* $f(N_H)$

As discussed in § 2.1, although accurate N_H determination is difficult in some regimes, an observational $f(N_H)$ curve can be measured. In this section we will discuss which model best fits the current data, considering cases A, B, B′, and C from § 5.3. Since the majority of this data is in the intermediate redshift range, we again focus on a redshift of 2.5 when making model predictions. In § 5.2 we derived $f(N_H)$ assuming a power law distribution (eq. [46]) of N_{tot}. Keeping this assumption, the data enable us to determine the normalization coefficient C_t and the value of P_{ext} that provide the best fit to the number of damped Lyα clouds, and Lyman limit systems, relative to the number of Lyα forest clouds.

In Figure 4 we show recent data from Hunstead et al. (1988) (solid circles) and from Rauch et al. (1992) (open circles) for Lyα forest clouds, from Sargent, Steidel, & Boksenberg (1989) for Lyman limit systems (solid circles), and from Lanzetta et al. (1991) for damped Lyα clouds (solid circles). In order to compare cases A–C we normalize all model curves to pass through the solid point at $\log N_H = 13.75$, $\log f(N_H) = -12.26$. At this point the number of systems should be measured fairly accurately because it is on the linear part of the curve of growth. Since for each case we have set P_{ext}/k and ϵ, equations (50) and (51) allow a model prediction for $f(N_H)$. In comparing to the data, we will focus on the point at $N_H = 10^{17.23}$ cm^{-2} (the lower end of the Lyman limit range where the shape of the break allows accurate determination of N_H) and on the damped Lyα regime.

In Figure 4a we compare $f(N_H)$ for cases A and B′. Both have $\epsilon = 2$, but different choices of P_{ext}/k. The dashed lines illustrate case A ($P_{ext}/k = 0.24$ cm^{-3} K) for dark matter parameter $\gamma = 0$ and 1. For the purpose of these figures we have chosen $E_\gamma = 25$ eV ($N_{crit} = 10^{18}$ cm^{-2}), but the gap will begin and end at lower N_H for a lower energy of incident photons. The gap in the Lyman limit range is illustrated just by descending vertical lines. We have not calculated the exact shape of the break, which is sure to be spectrum dependent, but Figure 1 is a schematic illustration of what we might expect. The $\gamma = 1$ curve comes close to passing through the lower Lyman limit point, but both case A curves predict a factor of ~ 10 excess of damped Lyα systems. Case B′, with $P_{ext}/k = 17$ cm^{-3} K fits the damped systems adequately, but the curve passes well below the Lyman limit point, which has been accurately determined.

In Figure 4b, we give model curves for examples with $\epsilon = 1.6$ (cases B and C). Since the gravity-dominated regime begins at $N_H = 10^{16}$ cm^{-2} for case B (and even later for case C) we cannot distinguish between curves with different dark-matter parameters. The dashed curve (case B) corresponds to the same pressure as case B′ in Figure 4*a*. Changing the slope of the total column density distribution from $\epsilon = 2$ to $\epsilon = 1.6$ allows a better fit of the Lyman limit point.

Of our four examples, case C (the solid line in Fig. 3*b*) provides the best-fit overall and is within reasonable error estimates of all data points. An ideal fit to the damped systems would require a choice of P_{ext}/k much larger than 366 cm^{-3} K, and this would exceed the *COBE* y-parameter constraints. Note that the Lyman limit point in the gap is below the line connecting the curves at either side. For this favored case (case C), the transition from the pressure dominated to the gravity-dominated regime occurs at close to the same N_H as the transition to optically thick slabs. For a Lyman limit system with $\log N_H = 17.5$, the neutral fraction $N_H/N_{tot} = 3.2 \times 10^{-3}$, with pressure contributing 82% of the inward force. At the transition ($N_H = 10^{18}$ cm^{-2}) the neutral fraction has increased to $N_{H1}/N_1 = 5.3 \times 10^{-3}$.

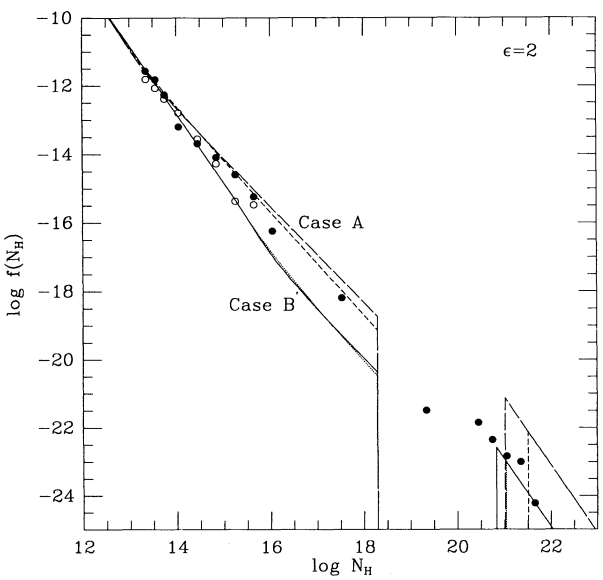

FIG. 4*a*

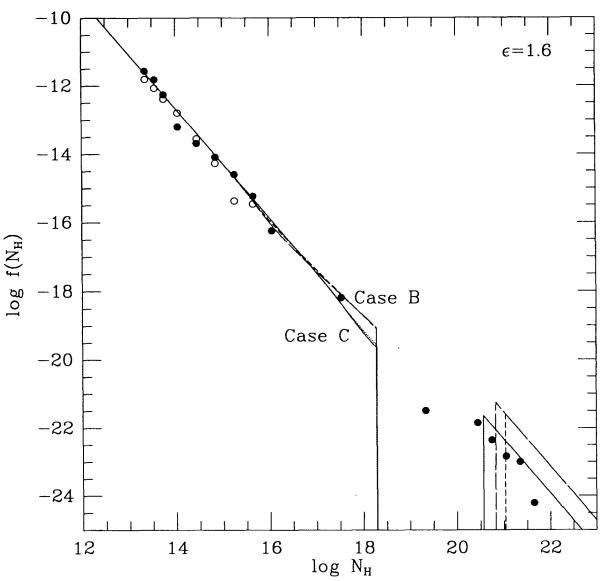

FIG. 4*b*

FIG. 4.—The solid points give the number of clouds observed per unit z by Hunstead et al. (1988) in the Lyα forest range, by Sargent et al. (1989) in the Lyman limit range, and by Lanzetta et al. (1991) in the damped range. The open circles represent similar data taken by Rauch et al. (1992) that should have somewhat better statistics than the earlier study. (*a*) A model with $\epsilon = 2$, with the value of P_{ext} chosen so that the curve passes through the third point. The upper curves are computed for the case A value of P_{ext}, while the lower ones are for case B′. In case A the long-dashed line represents $\gamma = 0$ and the short-dashed line, $\gamma = 1$. This dark matter parameter slightly affects the value of N_{crit}, the point at which the curves rise to begin the optically thick regime. (*b*) Two examples with $\epsilon = 1.6$, cases B and C. The transitions to the gravity-dominated regime are at larger values of N_H, so the differences produced by varying the dark matter parameter are not significant.

6. EVOLUTION OF SLABS

Until now, we have focused on the population of equilibrium slabs that would exist at a particular time (assuming the radiation and pressure incident on all slabs is equal). However, a given slab will adjust its properties as the extragalactic radiation field or the external pressure changes. (The slab distribution may also be affected by mergers or fragmentation, but we will neglect that effect here. This is almost certainly a safe assumption for the Lyα forest clouds, since they exhibit small correlations and typical separations greatly exceed their size.) The slab evolution can be described as a function of the following power-law indices: (1) ϵ, the index of the total column density spectrum of slabs as defined in equation (46); (2) γ, the dark-matter parameter defined in equation (38); (3) p, describing the evolution of the external pressure, $P_{\rm ext} \propto (1+z)^p$, where $p \leq 5$, and $p = 5$ is the adiabatic case; (4) j, describing the evolution of the radiation background, $\zeta \propto (1+z)^j$. The exponent j depends on cosmological effects and the adjustment of the spectrum due to absorbers, as well as the evolution of sources of radiation. For simplicity, in all numerical examples we will take j and p to be constant between $z = 2.5$ and the present. The evolution could proceed differently at higher z. The proximity effect indicates a relatively constant ζ at $z > 2.5$, but upper limits on the present-day extragalactic background radiation suggest a decline since then, with $j \gtrsim 3$.

As the external pressure decreases, the transition between pressure-dominated and gravity-dominated regimes will occur at smaller column densities. In the presence of significant dark matter (so we can use eq. [44]), we find that

$$N_1 \sim \left(\frac{1+z}{3.5}\right)^{p/(\gamma/2+1)}, \tag{58a}$$

$$\eta_1 \sim \left(\frac{1+z}{3.5}\right)^{p/[(\gamma/2-1)/(\gamma/2+1)]}. \tag{58b}$$

(As the transition shifts downward in total column density there will be a larger dark matter to gas ratio at the transition.) This total column density, N_1, corresponds to a neutral column density

$$N_{\rm H1} \sim \left(\frac{1+z}{3.5}\right)^{p[(\gamma/2+2)/(\gamma/2+1)]-j}. \tag{59}$$

Let us assume that we have data on Lyα forest clouds with a dominant contribution from $z = 2.5$ so that we can set $N_{\rm H1}$ at this redshift. Then equation (59) allows us to compute the shift of the transition between pressure and gravity confinement. Figure 5*a* illustrates the transition value of $N_{\rm H1}$ as a function of z for models corresponding to cases A, B, and C at $z = 2.5$ (see § 5.3). Above the curves slabs would be gravity confined and below they would be pressure confined. For the purpose of this example we have chosen $\gamma = 1$. The three different curves for each case have $(p = 5, j = 0)$, $(p = 5, j = 3)$, and $(p = 3.6, j = 3)$. (Above $z = 2.5$, ζ is taken to be constant, but cases with $p = 3.6$ and $p = 5$ are given.) For case A, the lowest $N_{\rm H}$ slabs are pressure confined at $z = 2.5$, but all observed Lyα clouds are gravity confined at present. Since the majority of observed forest clouds have $N_{\rm H}$ substantially below the Lyman limit, any equivalent width limited sample will be dominated by the lowest $N_{\rm H}$ clouds in the sample. If these are pressure confined, the evolution of the population of all clouds will be very similar whether the higher $N_{\rm H}$ clouds are gravity or pressure confined. Thus we can say that in case B, for $p = 5$ all observed clouds are gravity confined at present, while for $(p = 3.6, j = 3)$ evolution is dominated by the majority of clouds, which are pressure confined. For case C, we have chosen $P_{\rm ext}/k = 366$ cm^{-3} K at $z = 2.5$. With this value, favored by the considerations in § 5.4,

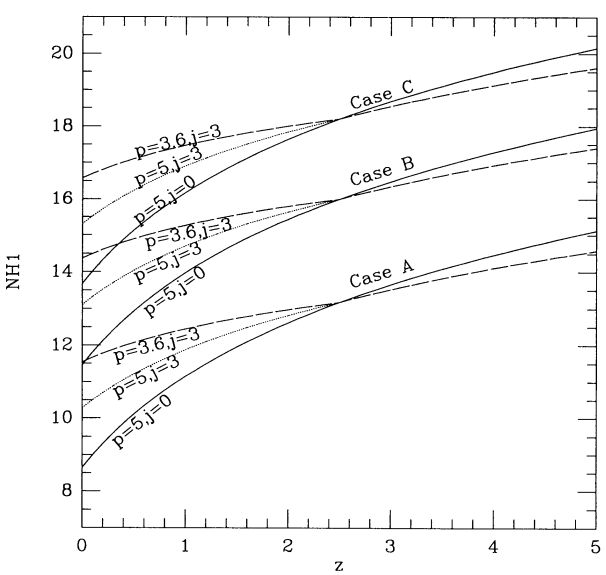

FIG. 5*a*

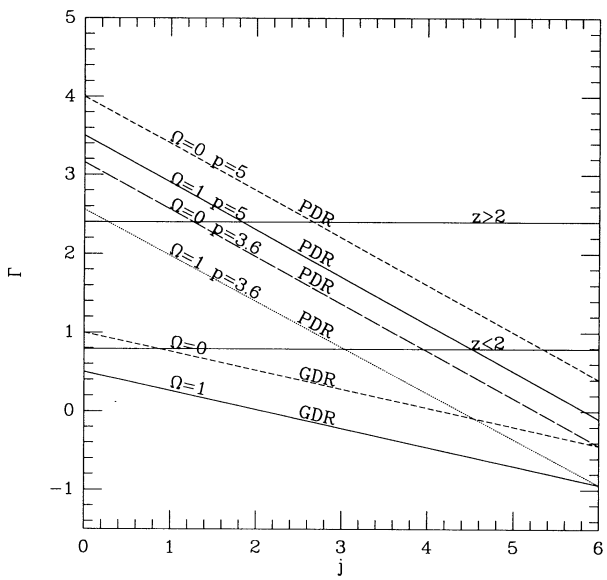

FIG. 5*b*

FIG. 5.—(*a*) The boundary between the pressure- and gravity-dominated regimes is illustrated as a function of redshift, for various models. The region above the curves is the gravity-dominated regime. Cases A, B, and C correspond to the values of $P_{\rm ext}$ specified in § 5.3 at $z = 2.5$. In all cases the dark matter parameters are $\eta_1 = 10$ and $\gamma = 1$. Above $z = 2.5$ we only illustrate constant ζ since this is suggested by observations, however, at lower z we demonstrate the effect of larger j. (*b*) The rate of change, for various models, of the extragalactic background radiation flux j that is needed to match observed Lyα forest cloud evolution Γ. The horizontal lines are the best observational values for clouds above and below $z = 2.5$, although error bars on these values are large.

all three choices of p and j lead to pressure confinement for most of the forest clouds, even at $z = 0$.

Due to cosmological effects, the distribution $g(N_{\rm tot})$ evolves as

$$g(N_{\rm tot}, z) \sim N_{\rm tot}^{-\epsilon}(1 + z)^{1-(\Omega_0/2)} \quad (60)$$

for $\Omega_0 = 0$ or 1 and a constant number of clouds per comoving volume. In general, $f(N_{\rm H}, z) \sim g[N_{\rm tot}(N_{\rm H}), z]\,(dN_{\rm tot}/dN_{\rm H})$. The evolution of the neutral column density for slabs with fixed $N_{\rm tot}$ is given by equations (39a), (40b), and (45b) as

$$N_{\rm H} \sim \frac{P_{\rm ext}}{\zeta} N_{\rm tot} \sim (1 + z)^{p-j}, \quad N_{\rm tot} \ll N_1, \quad (61a)$$

$$N_{\rm H} \sim \frac{1}{\zeta} N_{\rm tot}^{2+(\gamma/2)} \sim (1 + z)^{-j}, \quad N_{\rm tot} \gg N_1. \quad (61b)$$

If we define Γ such that the change in the number of clouds with a fixed $N_{\rm H}$ is $f(N_{\rm H}, z) \sim (1 + z)^{\Gamma}$, we can combine equations (60) and (61) to obtain

$$\Gamma = 1 - \frac{\Omega_0}{2} + (1 - \epsilon)(j - p), \quad N_{\rm H} \ll N_{\rm H1}, \quad (62a)$$

$$\Gamma = 1 - \frac{\Omega_0}{2} + \frac{(1 - \epsilon)j}{[2 + (\gamma/2)]}, \quad N_{\rm H} \gg N_{\rm H1}. \quad (62b)$$

If $\epsilon = 1.6$, we have $\Gamma = 1 - \Omega_0/2 - 0.6\,(p - j)$ in the pressure-dominated regime. This is very similar to equation (1) in Ikeuchi & Turner (1991), describing spherical pressure-confined clouds, with the slight difference due to the difference in geometry and their choice of $\epsilon = 1.5$. For comparison with their results we consider models with $p = 3.6$ and 5, and $\Omega_0 = 0$ and 1. The values of Γ for various models in the pressure-dominated regime, and in the gravity-dominated regime are given in Figure 5*b* which can be compared directly with Figure 1 in Ikeuchi & Turner (1991). The four pressure-confined models are very similar to that figure; however, clouds in the gravity-dominated regime evolve very differently.

Let us consider three specific examples corresponding to cases A, B, and C from § 5: (1) If we have $N_{\rm H1} = 1.5 \times 10^{13}$ cm^{-2} (case A) then all observed clouds are gravity confined at $z < 2.5$, and one of the lower two curves in Fig. 5*b* will apply. (For gravity-confined models, the evolution is independent of p). Comparing to the model curves for the gravity-dominated regime, the value $\Gamma = 2.4$ (for $z > 2.5$) only results for $j \ll 0$, i.e., a rapidly increasing radiation field with decreasing z. Even the observed low z evolution ($\Gamma = 0.8$) requires $j < 0$ for $\Omega_0 = 1$. (2) If we choose $N_{\rm H1} = 10^{16}$ cm^{-2} at $z = 2.5$ with $\epsilon = 1.6$ (case B) and $p = 5$ we will have Lyα forest clouds that are pressure confined at high z and gravity confined at low z. For $\Omega_0 = 1$, the high z evolution is fitted by $j = 0.3$ for $p = 3.6$, and by $j = 1.8$ for $p = 5$. Even for a fixed value of j there will be a tendency for Γ to decrease with decreasing z as more clouds become gravity confined. For gravity-confined clouds at present the observed Γ can be matched either for $\Omega = 1$ and $j = -1.3$ or for $\Omega = 0$ and $j = 0.8$. (3) If most clouds at all z are pressure confined (case C or possibly case B with $p = 3.6$ and large j), a decrease in Γ must result from an increase in j (as in Ikeuchi & Turner 1991). For $p = 5$, $\Omega_0 = 1$, and $\epsilon = 1.6$, $\Gamma = 0.8$ at $z = 0$ will result from $j = 4.5$, i.e., a factor of 281 decrease in ζ since $z = 2.5$, while for $p = 3.6$ the value $j = 3.1$ would be most consistent with this data.

It is unlikely that $j \sim 0$, so it is difficult to reconcile gravity-confined models with low z evolution. With $j \gtrsim 3$, models in which clouds are gravity confined at low z may slow the decrease in forest clouds too much, although it is possible that some intermediate case with a mixture of pressure and gravity confinement ($N_{\rm H1}$ near 10^{14} cm^{-2} at $z = 0$) could yield $\Gamma = 0.8$. Thus, based on the rate of evolution of the Lyα forest we conclude that case C is favored.

The evolution of the Lyα forest clouds provides information about whether pressure or gravity confinement is most important for $N_{\rm H} \sim 10^{14}$ cm^{-2}. In this section we demonstrated that only pressure confinement at $z > 2.5$ was consistent with the rapid evolution observed. At lower z pressure confinement with an ionization rate decreased substantially ($j \gtrsim 3$) since $z = 2.5$ will fit the data. Assuming $j = 4.5$ and $p = 5$, case C yields $P_{\rm ext}/k = 0.7$ cm^{-3} K, $\zeta = 10^{-14}$ s^{-1} (slightly smaller than the estimated attenuated quasar flux at present; Madau 1992). Equations (58) and (59) give the transition values of $N_{\rm H1} = 8.6 \times 10^{15}$ cm^{-2}, and $N_1 = 2.9 \times 10^{18}$ cm^{-2} at present. In this example, we set $\eta_1 = 10$ at $z = 2.5$ when $N_1 = 1.9 \times 10^{20}$ cm^{-2}, but equation (58b) gives $\eta_1 = 81$ at $z = 0$. If $N_{\rm H,crit} = 10^{18}$ cm^{-2}, we find from equation (52) that $N_{\rm crit} = 2.6 \times 10^{19}$ cm^{-2} at present, an order of magnitude larger than N_1. At $N_{\rm crit}$, well in the gravity-dominated regime, the ratio of dark matter to gas density is smaller than η_1, with $\eta(N_{\rm crit}) = 27$. For this dark matter density, the width of a slab with $N_{\rm tot} = N_{\rm crit}$ at $z = 0$ is 8.6 kpc.

7. H I EDGES OF GALACTIC DISKS AND Lyα CLOUDS ASSOCIATED WITH GALAXIES

So far we have considered Lyα clouds, with and without dark matter ($\eta \geq 1$), but all unrelated to galaxies. The portion of a gaseous spiral disk far outside of the stellar disk, with hydrogen column density $N_{\rm tot}$, shows some parallels and some differences. The external pressure $P_{\rm ext}$ and ionization rate ζ may be ubiquitous, and therefore the same around galaxies and Lyα forest clouds (at a given redshift). However, the dark matter for a disk portion is due to the whole galactic halo, so that η in equation (37) may be quite different than for isolated clouds. Furthermore, there may be magnetic and cosmic-ray pressure, or buoyancy, in the outskirts of a galaxy, so that T in equation (37) needs to be replaced by some "equivalent temperature" T^* which may be different from the gas kinetic temperature T_g. For an assumed η and T^*, calculations similar to those in § 5 can be performed for portions of the galactic disk. Two theoretical papers by Corbelli & Salpeter (1992) and Maloney (1993a) study this case in detail.

Observationally, Corbelli & Schneider (1990) and van Gorkom et al. (1992) (see van Gorkom 1991) have reported sharp H I edges in the galactic disks of M33 and NGC 3198. Specifically, they found that the H I column density $N_{\rm H}$ decreases slowly and smoothly with increasing radial distance until it reaches a value of $\sim 2 \times 10^{19}$ cm^{-2}, and then it drops suddenly to unobservable levels. For DDO 154 the column density at the edge is ~ 2 times smaller (Hoffman & Salpeter 1993). This effect is most naturally interpreted as the second transition in our § 5, i.e., the observed edge corresponds to $N_{\rm crit} \sim 2 \times 10^{19}$ cm^{-2}, with $N_{\rm H,crit} \sim 10^{18}$ cm^{-2} below the current observational threshold for H I (Sunyaev 1969; Felten & Bergeron 1969; Bochkorev & Sunyaev 1977; Corbelli & Salpeter 1992; Maloney 1993). With T^* in the equivalent to equation (37) unknown, and dark-matter gravity uncertain

(even for a known rotation curve) because the degree of flattening of the spheroidal halo is not known, there are many input parameters for the outer disk problem. One approach, taken by Corbelli & Salpeter (1992; following Merrifield 1992) is to assume that the model should yield a width of $W \sim 2$ kpc for $N_{crit} \sim (1\text{–}2) \times 10^{19}$ cm^{-2}. Assuming that P_{ext} is unimportant, and that the dark matter halo is spherical, they found $T^* \sim 2 \times 10^4$ K, $\eta \sim 20$, and $\zeta \sim (1 - 4) \times 10^{-14}$ s^{-1}.

In § 6, we discussed the evolution of the Lyα clouds, assuming that they were all separate from galaxies. The best fit to data on the absolute number of systems, and on the rate of evolution at low z, was provided by a model with a relatively large P_{ext} (case C with $p = 5$), and with a rapidly decreasing ionization rate ($j = 4.5$), resulting in $\zeta = 10^{-14}$ s^{-1} at present. The critical value of the total column density is $N_{crit} = 2.6 \times 10^{19}$ cm^{-2} (eq. [52b]), which is very close to the observed value for galaxy disks. We found at the end of § 6 that this example (with $\eta_1 = 10$) yielded $W_{eq} = 8.6$ kpc. These values are not all that dissimilar to those obtained by Corbelli & Salpeter (1992) from H I disks, although the width is significantly larger.

Presumably the gaseous disk extends out beyond the H I edge, mostly in ionized form, with N_H decreasing with radial distance below $N_{H,crit}$, thereby mimicking Lyα clouds below the "Lyman-edge" region into the forest region. It is possible that N_{tot} decreases more slowly than exponential (so that $N_H > 10^{13}$ cm^{-2} out to large radial distances), but more rapidly than the dark matter density, so that η (which was already large, ~ 80, at $N_{H,crit}$) becomes very large. Extended disks of present-day spiral or dwarf galaxies have already been invoked to produce the low-redshift Lyα lines (Maloney 1992). A more complicated hypothesis about cloud evolution from $z \sim 2.5$ to the present will be discussed in a later paper (Charlton et al. 1993).

Here we will only illustrate this hypothesis with a simple, but unrealistic, two population model which assumes that (1) most Lyα clouds observed at $z \gtrsim 2.5$ are indeed unassociated with ordinary galaxies and their η happens to vary little with z. (2) Some fraction f_g (e.g., 10%) of clouds with $N_{tot} \lesssim N_{crit}$ are in fact just portions of an outer galactic disk with the halo providing a fairly large η (e.g., 100). Let us take the external pressure P_{ext} to be large for $z \gtrsim 2.5$ so that the Lyα forest clouds are pressure dominated, even for $\eta \sim 100$. In that case N_H/N_{tot} is the same for $\eta \approx 1$ as for $\eta \sim 100$ and only the small fraction f_g of observed Lyα "clouds" are in ordinary galaxy disks. However, even at $z \sim 2.5$ clouds with N_H in the Lyman limit regime (N_H slightly less than $N_{H,crit}$) could be dark-matter dominated for $\eta \sim 100$, as may apply in galaxy outskirts. For such gravity confined clouds the density, and hence the neutral fraction N_H/N_{tot}, is much larger than for pressure-confined extragalactic clouds with $\eta \approx 1$. Although the fraction f_g for a given N_{tot} is just as small as at $z \gtrsim 2.5$, the much larger value of N_H coupled with the steepness of $g(N_{tot})$ will, for a given N_H, yield a much larger fraction of observed clouds that result from gas in galaxy outskirts. As discussed in § 6, P_{ext} is much smaller at $z \sim 0$ than at $z \sim 2.5$, and the transition from pressure to gravity domination occurs at a lower column density N_1. Even Lyα forest clouds may then be gravity dominated for $\eta \sim 100$ (but not for $\eta \approx 1$) and therefore may be more likely to be observed from "clouds" in galaxies than from extragalactic ones. This could explain the Bahcall et al. (1993) observation of several forest clouds that appear to be closely associated with low z galaxies, in contrast to the lack of correlations between these clouds at high z.

8. SUMMARY AND DISCUSSION

We have explored solutions for the equilibrium configuration of a slab with ionizing radiation incident equally from both sides. In this study of parameter space, we included radiation effects (photoionization, Lyα photon trapping, and mock gravity) as well as external pressure, and self-gravity (with and without dark matter). We applied the general formalism first to structure growth on small scales at very high z due to mock gravity on dust. Such a mechanism may have a significiant effect on growth of structure (compression of slabs) if the incident ionizing radiation field is strong, and if small amounts of dust (a first generation of stars) have already been produced. The time scale for contraction by a factor of 2 is not very much smaller than a Hubble time, and the radiation required comes close to violating *COBE* FIRAS constraints, but these models cannot at the moment be ruled out.

Our emphasis has been on the application to slab models at $z < 5$, particularly those that may correspond to Lyα forest, Lyman limit, and damped Lyα systems. The equilibrium is then a balance of the inward forces of gravity and external pressure, and the outward force of gas pressure. The value of the external pressure and the amount of dark matter set a value of N_H, the neutral H column density, at which a transition occurs, between a regime where external pressure is the dominant inward force, and one where gravity confines the slabs. Below this transition, N_H increases linearly with total H column density N_{tot} (including ionized and neutral forms). Above the transition, $N_H \sim N_{tot}^3$ if there is no dark matter, or $N_H \sim N_{tot}^{2-3}$ depending on the form of the dark matter distribution. This transition will lead to a feature in the distribution of the number of clouds with N_H, $f(N_H)$. The predicted direction of the break in the function $f(N_H)$ is such that there is a steeper rise toward small N_H. The data, which have a dominant contribution from clouds at $z \sim 2.5$, do not yet allow identification of this transition. Theoretically it could occur anywhere, over many orders of magnitude in N_H. A IGM pressure P_{ext}/k of 0.03 cm^{-3} K ($\Omega_{ext} T_{ext} \sim 100$ at $z \sim 2.5$) will lead to a break below the N_H of observable Lyα forest clouds. However, if the value is as large as $P_{ext}/k \sim 100$ cm^{-3} K ($\Omega_{ext} T_{ext} \sim 5 \times 10^5$ at $z \sim 2.5$) the break will occur at $N_H > 10^{17}$ cm^{-2} in the Lyman limit range. An intermediate value of P_{ext} should eventually be apparent as the observed $f(N_H)$ for clouds at $z \gtrsim 2.5$ is refined. This would be a direct measurement of P_{ext}. If a flattening at low N_H (such as suggested by Carswell et al. [1984] and Webb et al. [1992] should be confirmed, this could only be explained by a change in the distribution of total column density $g(N_{tot})$, i.e., fewer loss-mass clouds then predicted by a power-law extrapolation, a relic of the formation process of the clouds.

A second transition will begin when N_H is large enough that the slab becomes optically thick to ionizing radiation at 13.6 eV, and gradually approaches a configuration with a neutral center sandwiched by ionized layers. At the highest N_H, when the optical depth to the spectrum of radiation exceeds one, we expect $N_H = N_{tot}$. Since N_H increases rapidly, from the value at the start of the transition to N_{tot}, there is a lack of clouds (a "gap") in the distribution $f(N_H)$ of neutral column densities in this range. This gap has not been observed at the lower end of the Lyman limit regime, indicating that the ionizing radiation has a dominant component at energies somewhat larger than 13.6 eV.

Current uncertainties in the observed distribution $f(N_H)$ do not allow measurement of the external pressure by identifica-

tion of a break. However, assuming the distribution $g(N_{tot})$ is a power law from the Lyα forest up through damped systems we can estimate P_{ext} based on the relative numbers of forest and damped Lyα clouds. This yields a best fit value of $P_{ext}/k = 366$ cm^{-3} at $z = 2.5$ (case C in § 5.3). Although we expect a power-law distribution of N_{tot} to hold over some range of N_H, it is clear that there will be some upper and lower mass limit. (In a given formation model the mass must determine the longer dimensions of the slab, as well as N_{tot}. The observed $g(N_{tot})$ (as opposed to the actual distribution of perpendicular N_{tot} of slabs) must also include the more frequent occurrence of slabs with a larger surface area.) When we compute the number of damped systems expected, e.g., in the case A or case B models, we are assuming the power law $g(N_{tot})$ to hold up to the maximum observed N_H.

A source of error in this estimate of P_{ext} is that the number of systems may have been measured incorrectly. On the Lyα forest end the number of clouds could be underestimated as a result of line blending, leading to a larger best-fit value of P_{ext}. For damped Lyα systems, Pei & Fall (1992) have estimated that dust obscuration may substantially reduce the number of observed systems, so that the best fit to the corrected number would yield a smaller P_{ext}/k.

One of the standard questions concerning the Lyα clouds is their contribution to the total mass density of the universe. For our models, the general expressions for the cloud contribution of Ω_0 are given in equations (47) and (48). For the extreme value of $\epsilon = 2$, the contribution is equal for equal logarithmic intervals in total column density. This corresponds either to the same (pressure-dominated) or a much larger (gravity-dominated) interval in N_H. For a smaller ϵ, the lower end of the mass spectrum has a smaller contribution to Ω_0. Although the lower mass cutoff is uncertain (compared to the upper end that is set by the largest damped clouds) the value Ω_{cl} is almost independent of N_{min}. Our range of models predicts $0.0005 \lesssim \Omega_{cl} \lesssim 0.01$, small compared to the baryonic density contribution derived from nucleosynthesis ($\Omega_b \sim 0.02$; Walker et al. 1991). The largest contribution to the baryon density is likely come from the IGM for models with a large value of P_{ext} (such as case C).

The ionizing background radiation and the external pressure are likely to change with z. As P_{ext} decreases (the IGM cools), the transition from pressure to gravity domination will gradually shift to smaller values of N_H. Changes in ζ and P_{ext} will also alter the relationship between N_H and N_{tot}, and thus $f(N_H)$ will change with time. In all of the discussion of cloud evolution we have assumed that the surface area of a cloud is fixed, i.e., the long dimension does not change. Such a change would alter $g(N_{tot})$, which we take as fixed with time. In both the pressure- and gravity-dominated regimes, we have derived the relationship between slab evolution [$f(N_H, z) \sim (1 + z)^{\Gamma}$] and the change in the ionization rate [$\zeta \sim (1 + z)^j$] for a given p[$P_{ext} \sim (1 + z)^p$].

The evolution can be used as a means to place limits on P_{ext}. If P_{ext} is small then the slabs will be gravity confined and an unrealistically rapid increase in ionizing radiation is needed to match observations of $\Gamma \sim 2.4$ at $z \sim 2.5$. This suggests that P_{ext} substantially exceeds 0.8 cm^{-3} K at $z = 2.5$, so that pressure-confined clouds have dominant contribution to the evolution. The low z evolution ($\Gamma \sim 0.8$) can be consistent either with a pressure-confined Lyα forest with ζ substantially decreased since $z = 2.5$ or with gravity-confined clouds with a much smaller decrease in ζ. Consideration of the proximity effect and high-velocity clouds indicate that ζ has decreased since $z = 2.5$. This may be inconsistent with low z evolution if all forest clouds are gravity confined. For pressure-confined clouds with $\Omega_0 = 1$ and $p = 5$, the low z evolution from $z \sim 2.5$ to $z \sim 0$ is best fitted by $j \sim 4.5$, or $\zeta \sim 10^{-14}$ s^{-1}. For $p = 3.6$, we obtained $j = 3.1$. Uncertainties in this consideration include the relation between N_H and equivalent width (used to derive Γ), and the assumption of a single population of clouds.

We have just described three considerations related to the statistics of the population of Lyα clouds: (1) the relative numbers of forest, Lyman limit, and damped clouds, (2) the rate of evolution of the Lyα forest at high z, and (3) the rate of evolution of the Lyα forest at low z. Each consideration can be used to constrain model parameters, particularly the pressure of the IGM and rate of change of the extragalactic background radiation. However, the results are indefinite due to observational uncertainties and to various assumptions such as a power-law total column density distribution, a lack of dust obscuration of damped Lyα clouds, and that forest clouds at high and low z are the same population. Although many models are possible, particularly with relaxed assumptions, we choose the model with $P_{ext}/k = 366$ cm^{-3} K at $z = 2.5$, $p = 5$ ($P_{ext}/k \sim 1$ cm^{-3} K at present), $\Omega_{cl} \sim 10^{-3}$, and $j = 4.5$ ($\zeta \sim 10^{-14}$ s^{-1} at present) as an example that fits all the data fairly well within uncertainties. Alternatively, if $p = 3.6$, then j could be smaller and the present-day value of ζ would exceed the estimated quasar contribution.

Our general formulae describing the equilibrium configuration of a slab included the possibility of dark matter. In the examples, throughout we have usually adopted a modest amount of dark matter ($\eta_1 = 10$). Since $N_{H1} \sim \eta_1^{1/2}$, the transition from pressure- to gravity-domination varies for models with different amounts of dark matter. For example, if there were no dark matter the transition from pressure to gravity domination would occur at an N_{H1} that is a factor of 3 smaller than the $\eta_1 = 10$ case. However, a factor of 3 shift makes little qualitative difference over many orders of magnitude in N_H. Similarly, the amount and distribution of dark matter makes little qualitative difference to the rate of cloud evolution. Referring to Figures 2*b* and 3*b*, we see that the addition of dark matter can change predictions of slab widths by as much as an order of magnitude. As a final example of the effect of dark matter, we consider case B in Figure 4*a*. This moderate pressure case fits the damped Lyα data, but falls well short of the Lyman limit point. Although an increase in the amount of dark matter will adjust the curve relative to this point, a factor of 1000 increase in η_1 would be needed for a good fit. Thus a smaller P_{ext} with a larger ϵ and more dark matter is not an adequate solution.

We would like to know how certain we can be that P_{ext} is large. For example, if a break was identified at $N_{H1} = 10^{13}$–10^{14} cm^{-2} in the $f(N_H)$ distribution, indicating a smaller P_{ext}, could this be reconciled with the other observations in the context of these models? From Figure 4*a*, we see that we would need to resort to dust obscuration of damped Lyα clouds, or an adjustment of $g(N_{tot})$ at the high end to fit the $f(N_H)$ distribution. Also, a rapid decrease in the number of clouds at $z = 2.5$ is difficult to explain with purely gravity confined clouds (see Fig. 5*b*) so there seems to be a discrepancy here. The low z evolution required a value of $j \sim 0$–1 averaged from $z = 2.5$ until the present. There may be a problem reconciling the small j with other indications that ζ has decreased substantially since $z = 2$, but the proximity effect value is probably sufficiently

uncertain as to allow this. Nonetheless it seems unlikely that the conventional single population slab model allows such a small P_{ext}.

Certain of the considerations in this paper assume that the Lyα clouds are a single population distinct from galaxies. Yet, it is clear that spiral galaxy disks also have neutral column densities that would produce a Lyα absorption line in a QSO spectrum. In § 7, we discussed the parallels between the H I disk of a spiral galaxy as we proceed outward in radius, and the progression from damped Lyα, to Lyman limit, to Lyα forest clouds. Observations of outer disks of spiral galaxies show a rapid decrease in the neutral column density at N_H of order 2×10^{19} cm^{-2}, presumably due to the transition from the optically thin to the optically thick regime. If we assume that this disk has the same geometry, dark matter density, external pressure, and ionization rate, as the isolated Lyα forest clouds, our formalism will apply to this situation as well. Our favored model (case C), for a slab that becomes optically thick at $N_H = 10^{18}$ cm^{-2}, predicts that the critical value of the total column density N_{crit} is 2.6×10^{19} cm^{-2}, and the slab width W is 8.6 kpc. However, the ratio of dark matter to gas density could be larger in the outer regions of spiral disks, leading to a smaller N_{crit} and W. With such a scheme, it is possible that most Lyα clouds observed at $z \sim 2.5$ would be isolated systems in the pressure-dominated regime, while at $z \sim 0$ there would be a large contribution from lines of sight through galaxy disks (see also Maloney 1992). The latter could be gravity confined, although their isolated companions with the same N_H may still be contained by IGM pressure. The result of this two-population model is a larger predicted number of clouds at low redshift relative to the single-population model. Thus consistency with the Bahcall et al. (1992) measurement of the number of forest clouds at $z \sim 0$ could possibly be attained without resorting to such large values of j. A forthcoming paper (Charlton et al. 1993) will give details of this model and of a variant where most of the nonclustered Lyα clouds at $z \sim 2.5$ are precursors of "faint blue galaxies" (Babul & Rees 1992), which subsequently lose much of their gas in a galactic wind.

The relatively large P_{ext}/k suggested by the various considerations in this paper is consistent with the *COBE* y-parameter constraints, but requires a large IGM temperature to be consistent with Gunn-Peterson limits. For example, the case C pressure ($P_{ext}/k \sim 300$ cm^{-3} K at $z \sim 2.5$) would require $T \gtrsim 10^7$–10^8 K at high z. Some early heating process is then required, such as shock heating due to explosions, galactic winds, or supercluster formation. The total mass required in the hot external gas (see eq. [6]) is quite large, e.g., $\Omega_{ext} > 0.01$ for case C (more than could be obtained by galactic winds from all faint blue galaxies).

Our goal in this study was to present a general set of formulae to describe the equilibrium configuration of a slab of hydrogen. We have demonstrated how this formalism can be applied to predict the properties of the population of Lyα clouds for any choice of the model parameters. At the moment, comparing our various models with the available observational information tentatively suggests that the pressure of the IGM is rather large and that the ionization rate decreases fairly rapidly with time since $z \sim 2.5$. However, the models also allow detailed predictions for future observations. We can be alert to any changes of slope of the distribution $f(N_H)$, which could indicate a pressure to gravity domination transition if the curve steepens at small N_H, or a lower mass cutoff if it flattens. The evolution of Lyα forest clouds as a function of equivalent width can be predicted for any model and compared to observations that consider bins in equivalent width (Bechtold 1992). As better statistics become available for evolution of the column density distribution from $z \sim 2.5$ to $z \sim 0$, and on the association of low z forest clouds with galaxies, we can make more definite comparisons.

This work was supported by NSF grants AST88-22297 at Steward Observatory of the University of Arizona, AST-91-19475 at Cornell University and NASA grants NAGW-2569 and NAGW-2523 at the University of Washington. Two of us (J. C. C. and C. J. H.) would like to acknowledge the Aspen Center for Physics where discussions related to this paper took place. We would also like to thank J. Bechtold, J. Black, A. Burrows, E. Corbelli, A. Dobrzycki, L. Hoffman, P. Madau, P. Meszaros, P. J. E. Peebles, R. Romani, P. Schinder, and J. Webb for their insights into this project.

REFERENCES

Atwood, B., Baldwin, J. A., & Carswell, R. F. 1985, ApJ, 292, 58
Babul, A., & Rees, M. J. 1992, MNRAS, 255, 346
Bahcall, J. N., Jannuzi, B. T., Schneider, D. P., Hartig, G. F., Bohlin, R., & Junkkarinen, V. 1991, ApJ, 377, L5
Bahcall, J. N., Jannuzi, B. T., Schneider, D. P., & Hartig, G. F. 1993, ApJ, submitted
Bahcall, J. N., Jannuzi, B. T., Schneider, D. P., Hartig, G. F., & Green, R. F. 1992, ApJ, 397, 68
Bajtlik, S., Duncan, R. C., & Ostriker, J. P. 1988, ApJ, 327, 570
Barcons, X., & Fabian, A. C. 1987, MNRAS, 224, 675
Barcons, X., & Webb, J. K. 1991, MNRAS, 253, 207
Baron, E., Carswell, R. F., Hogan, C. J., & Weymann, R. J. 1989, ApJ, 337, 609
Bechtold, J. 1991, private communication
———. 1993, ApJ, submitted
Bechtold, J., Weymann, R. J., Lin, Z., & Malkan, M. A. 1987, ApJ, 215, 180
Binney, J., & Tremaine, S. 1987, Galactic Dynamics (Princeton Univ. Press), 313
Black, J. H. 1981, MNRAS, 197, 553
———. 1991, private communication
Bochkorev, N. G., & Sunyaev, R. A. 1977, Soviet Astron.–AJ, 21, 5
Bond, J. R., Carr, B. J., & Hogan, C. J. 1991, ApJ, 367, 420
Bond, J. R., Szalay, A. S., & Silk, J. 1988, ApJ, 324, 627
Bonilha, J. R. M., Ferch, R., Salpeter, E. E., Slater, G., & Noerdlinger, P. D. 1979, ApJ, 233, 649
Braun, E., & Dekel, A. 1989, ApJ, 345, 31
Carilli, C. L., van Gorkom, J. H., & Stoke, J. T. 1989, Nature, 338, 134
Carswell, R. F., Lanzetta, K. M., Parnell, H. C., & Webb, J. K. 1991, ApJ, 371, 36
Carswell, R. F., Morton, D. C., Smith, M. G., Stockton, A. N., Turnshek, D. A., & Weymann, R. J. 1984, ApJ, 278, 486
Cen, R., & Ostriker, J. P. 1991, August IGM Workshop
Chaffee, F. H., Foltz, C. B., Bechtold, J., & Weymann, R. J. 1986, ApJ, 301, 116
Charlton, J. C., Corbelli, E., Hoffman, G. L., & Salpter, E. E. 1993, in preparation
Cheng, E. 1991, BAAS, 23, 896
Colgan, S. W. J., Salpeter, E. E., & Terzian, Y. 1990, ApJ, 351, 503
Corbelli, E., & Salpeter, E. E. 1993, ApJ, submitted
Corbelli, E., & Schneider, S. E. 1990, ApJ, 356, 14
Donahue, M., & Shull, J. M. 1991, ApJ, 383, 511
Duncan, R. C., Vishniac, E. T., & Ostriker, J. P. 1991, ApJ, 368, L1
Felten, J. E., & Bergeron, J. 1969, Astrophys. Lett., 4, 155
Field, G. B. 1971, ApJ, 165, 29
———. 1976, in Stars and Stellar Systems, ed. A. Sandage, M. Sandage, & J. Kristian (Univ. of Chicago Press), 375
Fukugita, M., & Lahav, O. 1991, MNRAS, 253, 17P
Hauser, M. G., Kelsall, T., Moseley, S. H., Silverberg, R. F., Murdoch, T., Toller, G., Spiesman, W., & Weiland, J., in After the First Three Minutes, ed. S. S. Holt, C. L. Bennett, & V. Trimble (New York: AIP), 161
Hoffmann, G. L., & Salpeter, E. E. 1993, in preparation
Hogan, C. J. 1987, ApJ, 316, L59
———. 1989, ApJ, 340, 1
Hogan, C. J., & White, S. D. M. 1986, Nature, 321, 575
Hunstead, R. W., Murdoch, H. S., Pettini, M., & Blades, J. C. 1988, ApJ, 329, 527
Ikeuchi, S., & Ostriker, J. P. 1986, ApJ, 301, 522
Ikeuchi, S., & Turner, E. L. 1991, ApJ, 381, L1

Jenkins, E. B., Bajtlik, S., & Dobrzycki, A. 1993, in preparation
Jenkins, E. B., & Ostriker, J. P. 1991, ApJ, 376, 33
Kutyrev, A. S., & Reynolds, R. J. 1989, ApJ, 344, L9
Lahav, L., Loeb, A., & McKee, C. F. 1990, ApJ, 349, L9
Lake, G. 1988, ApJ, 327, 99
Lanzetta, K. M. 1991, ApJ, 375, 1
Lanzetta, K. M., Turnshek, D. A., & Wolfe, A. M. 1987, ApJ, 322, 739
Lanzetta, K. M., Wolfe, A. M., Turnshek, D. A., Lu, L., McMahon, R. G., & Hazard, C. 1991, ApJS, 77, 1
Lu, L. 1991, ApJ, 379, 99
Madau, P. 1991, ApJ, 376, L33
———. 1992, ApJ, 389, L1
Maloney, P. 1992, ApJ, 398, L89
Maloney, P. 1993, ApJ, submitted
Mather, J. C., et al. 1990, ApJ, 354, L37
Merrifield, M. R. 1992, AJ, 103, 1553
Miralda-Escude', J., & Ostriker, J. P. 1990, ApJ, 350, 1
Morris, S. L., Weymann, R. J., Savage, B. D., & Gilliland, R. L. 1991, ApJ, 377, L21
Ostriker, J. P., & Ikeuchi, S. 1983, ApJ, 268, L63
Peebles, P. J. E. 1991, Aspen Summer Physics Workshop
Pei, Y. C., Fall, S. M., & Bechtold, J. 1991, ApJ, 378, 6
Pettini, M., Hunstead, R. W., Smith, L. J., & Mar, D. P. 1991, MNRAS, 246, 545
Rauch, M., Carswell, R. F., Chaffee, F. H., Foltz, C. B., Webb, J. K., Weymann, R. J., Bechtold, J., & Green, R. F. 1992, ApJ, 390, 387
Rees, M. J. 1986, MNRAS, 218, 25p
Reynolds, R. J. 1990, in The Galactic and Extragalactic Background Radiation, ed. S. Bowyer & C. Leinert (Dordrecht: Kluwer), 157
Sargent, W. L. W., Boksenberg, A., & Steidel, C. C. 1988, ApJS, 68, 539
Sargent, W. L. W., Steidel, C. C., & Boksenberg, A. 1989, ApJS, 69, 703
Sargent, W. L. W., Young, P. J., Boksenberg, A., & Tytler, D. 1980, ApJS, 42, 41
Schneider, D. P., Schmidt, M., & Gunn, J. E. 1989, AJ, 98, 1951
Shapiro, P. R., & Giroux, M. L. 1987, ApJ, 321, L107
Smette, A., Surdej, J., Shaver, P. A., Foltz, C. B., Chaffee, F. H., Weymann, R. J., Williams, R. E., & Magain, P. 1992, ApJ, 389, 39
Spitzer, L. 1941, ApJ, 94, 232
Steidel, C. C. 1990, ApJS, 72, 1
———. 1991, August IGM meeting
Steidel, C. C., & Sargent, W. L. W. 1987, ApJ, 318, L11
Sunyaev, R. A. 1969, Soviet Astron.–AJ, 13, 5
Tytler, D. 1987, ApJ, 321, 49
van Gorkom, J. H. 1991, in Atoms, Ions and Molecules: New Results in Spectral Line Astrophysics, ed. A. D. Haschick & P. T. P. Ho (San Francisco: ASP), 1
van Gorkom, J. H., Cornwell, T., van Albada, T. S., & Sancisi, R. 1993, in preparation
Vishniac, E. T., & Bust, G. S. 1987, ApJ, 319, 14
Walker, T. P., Steigman, G., Schramm, D. N., Olive, K. A., & Kang, H. 1991, ApJ, 376, 51
Wakker, B. P., Vijfschaft, B., & Schwarz, U. J. 1991, A&A, 249, 233
Webb, J. K., & Barcons, X. 1991, MNRAS, 250, 270
Webb, J. K., Barcons, X., Carswell, R. F., & Parnell, H. C. 1992, MNRAS, 255, 319
Williger, G. M., & Babul, A. 1992, preprint
Womble, D., Junkkarinen, V. T., & Burbidge, E. M. 1992, ApJ, 388, 55